leprae inhibits dendritic cell activation and maturation. *J. Immunol.* 178(1), 338–344 (2007).

•• **Evidence of *M. leprae* suppressing immune function.**

114 Karat AB, Job CK, Rao PS. Liver in leprosy: histological and biochemical findings. *Br. Med. J.* 1(5744), 307–310 (1971).

•• **Histological findings and their correlation with biochemical functions of the liver in leprosy patients.**

115 Sehgal VN, Tyagi SP, Kumar S, Gupta MC, Hameed S. Microscopic pathology of the liver in leprosy patients. *Int. J. Dermatol.* 11(3), 168–172 (1972).

116 Crispe IN. Hepatic T cells and liver tolerance. *Nat. Rev. Immunol.* 3(1), 51–62 (2003).

117 Crispe IN. The liver as a lymphoid organ. *Annu. Rev. Immunol.* 27, 147–163 (2009).

•• **Important discussion of the immunological role of the liver.**

118 Crispe IN, Dao T, Klugewitz K, Mehal WZ, Metz DP. The liver as a site of T-cell apoptosis: graveyard, or killing field? *Immunol. Rev.* 174, 47–62 (2000).

119 Dienstag JL. Hepatitis B virus infection. *N. Engl. J. Med.* 359(14), 1486–1500 (2008).

120 Sunderkotter C, Nikolic T, Dillon MJ *et al.* Subpopulations of mouse blood monocytes differ in maturation stage and inflammatory response. *J. Immunol.* 172(7), 4410–4417 (2004).

121 Yogi Y, Banba T, Kobayashi M *et al.* Leprosy in hypertensive nude rats (SHR/NCrj-rnu). *Int. J. Lepr. Other Mycobact. Dis.* 67(4), 435–445 (1999).

122 Dagur PK, Sharma B, Kumar G *et al.* Mycobacterial antigen(s) induce anergy by altering TCR- and TCR/CD28-induced signalling events: insights into T-cell unresponsiveness in leprosy. *Mol. Immunol.* 47(5), 943–952 (2010).

123 Rojas-Espinosa O, Estrada-Parra S. Immunology of leprosy: cellular anergy to *Mycobacterium leprae*. *Arch. Invest. Med. (Mex.)* 20(4), 335–341 (1989).

JCM
Journals.ASM.org

Discrimination of *Mycobacterium abscessus* subsp. *massiliense* from *Mycobacterium abscessus* subsp. *abscessus* in Clinical Isolates by Multiplex PCR

Kazue Nakanaga,[a] Tsuyoshi Sekizuka,[b] Hanako Fukano,[c] Yumi Sakakibara,[a] Fumihiko Takeuchi,[b] Shinpei Wada,[c] Norihisa Ishii,[a] Masahiko Makino,[a] Makoto Kuroda,[b] Yoshihiko Hoshino[a]

Leprosy Research Center, National Institute of Infectious Diseases, Tokyo, Japan[a]; Pathogen Genomics Center, National Institute of Infectious Diseases, Tokyo, Japan[b]; School of Veterinary Medicine, Nippon Veterinary and Life Science University, Tokyo, Japan[c]

The rapidly growing mycobacterium *M. abscessus sensu lato* is the causative agent of emerging pulmonary and skin diseases and of infections following cosmetic surgery and postsurgical procedures. *M. abscessus sensu lato* can be divided into at least three subspecies: *M. abscessus* subsp. *abscessus*, *M. abscessus* subsp. *massiliense*, and *M. abscessus* subsp. *bolletii*. Clinical isolates of rapidly growing mycobacteria were previously identified as *M. abscessus* by DNA-DNA hybridization. More than 30% of these 117 clinical isolates were differentiated as *M. abscessus* subsp. *massiliense* using combinations of multilocus genotyping analyses. A much more cost-effective technique to distinguish *M. abscessus* subsp. *massiliense* from *M. abscessus* subsp. *abscessus*, a multiplex PCR assay, was developed using the whole-genome sequence of *M. abscessus* subsp. *massiliense* JCM15300 as a reference. Several primer sets were designed for single PCR to discriminate between the strains based on amplicons of different sizes. Two of these single-PCR target sites were chosen for development of the multiplex PCR assay. Multiplex PCR was successful in distinguishing clinical isolates of *M. abscessus* subsp. *massiliense* from samples previously identified as *M. abscessus*. This approach, which spans whole-genome sequencing and clinical diagnosis, will facilitate the acquisition of more-precise information about bacterial genomes, aid in the choice of more relevant therapies, and promote the advancement of novel discrimination and differential diagnostic assays.

Members of the *Mycobacterium chelonae-M. abscessus* group of rapidly growing mycobacteria (RGM), *M. abscessus sensu lato*, have been identified not only as sources of pulmonary infections but also as emerging pathogens of nosocomial infections following cosmetic surgery and postsurgical procedures (1–4). The taxonomic status of *M. abscessus sensu lato* has not been resolved; however, *M. massiliense* and *M. bolletii* were characterized as new species distinct from *M. abscessus* (5, 6). Although the clinical significance of *M. massiliense* has been emphasized (7, 8), it was proposed by Leao et al. in 2011 that *M. massiliense* and *M. bolletii* should be reclassified as a united subspecies of *M. abscessus*, *M. abscessus* subsp. *bolletii*, and that a new subspecies, *M. abscessus* subsp. *abscessus*, should be designated (9). However, a recent whole-genome study strongly supported the hypothesis that the species can be divided into at least three subspecies: *M. abscessus* subsp. *abscessus*, *M. abscessus* subsp. *massiliense*, and *M. abscessus* subsp. *bolletii* (10). *M. abscessus* subsp. *massiliense* was initially isolated from the sputum of a patient with pneumonia in France in 2004 (5). In 2005, an outbreak of *M. abscessus* subsp. *massiliense* infection was linked to intramuscular injections of an antimicrobial agent in South Korea (11). This bacterium was also the source of a lethal case of sepsis in Italy (12) and has been found in cystic fibrosis patients in France (13). Several cases of bacteremia and cutaneous pulmonary infections have also been reported in Japan (14–17).

A novel approach is required to differentiate *M. abscessus* subsp. *massiliense* from *M. abscessus* subsp. *abscessus* and *M. abscessus* subsp. *bolletii* because conventional methods such as biochemical assays and 16S rRNA genotyping cannot make the discrimination. Moreover, the clinical profile of *M. abscessus* subsp. *massiliense* is different from those of *M. abscessus* subsp. *abscessus* and *M. abscessus* subsp. *bolletii*. In particular, antibiotic treatment with clarithromycin is more effective against *M. abscessus* subsp. *massiliense* lung infections, with resistance developing more readily in cases of *M. abscessus* subsp. *abscessus* lung disease. Therefore, differentiating *M. abscessus* subsp. *massiliense* from *M. abscessus* subsp. *abscessus* is critical in the clinical environment (7). A significant difference between *M. abscessus* subsp. *massiliense* and *M. abscessus* subsp. *abscessus-M. abscessus* subsp. *bolletii* in susceptibility to various antimycobacterial drugs has also been observed in our laboratory (17). A significant difference between *M. abscessus* subsp. *abscessus* and *M. abscessus* subsp. *massiliense* in treatment response was also noted (18). However, the incidence of *M. abscessus* subsp. *bolletii* infection is very rare, making it difficult to separate its clinical profile from that of an *M. abscessus* subsp. *abscessus* infection.

In Japanese hospitals, a commercially available DNA-DNA hybridization (DDH) assay is frequently used for the clinical identi-

Received 24 May 2013 Returned for modification 23 June 2013
Accepted 1 November 2013
Published ahead of print 6 November 2013
Editor: K. C. Carroll
Address correspondence to Kazue Nakanaga, nakanaga@nih.go.jp, or Makoto Kuroda, makokuro@nih.go.jp.
K.N. and T.S. contributed equally to this article.
Supplemental material for this article may be found at http://dx.doi.org/10.1128/JCM.01327-13.
Copyright © 2014, American Society for Microbiology. All Rights Reserved.
doi:10.1128/JCM.01327-13

Downloaded from http://jcm.asm.org/ on December 20, 2013 by NATL INST OF INFECTIOUS DISEAS

TABLE 1 Primers used in this study

Primer	Sequence	Target and/or purpose (amplified fragment size)	Reference
8F16S	5′-AGAGTTTGATCCTGGCTCAG-3′ (positions 8 to 27)[a]	Mycobacterial 16S rRNA gene, PCR (ca. 1,500 bp), sequencing	21
1047R16S	5′-TGCACACAGGCCACAAGGGA-3′ (positions 1047 to 1028)[a]		
830F16S	5′-GTGTGGGTTTCCTTCCTTGG-3′ (positions 830 to 849)[a]		
1542R16S	5′-AAGGAGGTGATCCAGCCGCA-3′ (positions 1542 to 1523)[a]		
TB11	5′-ACCAACGATGGTGTGTCCAT-3′	Mycobacterial *hsp65* gene, PCR (441 bp), sequencing	22
TB12	5′-CTTGTCGAACCGCATACCCT-3′		
MabrpoF	5′-GAGGGTCAGACCACGATGAC-3′ (positions 2112–2131)[b]	Mycobacterial *rpoB* gene, PCR (449 bp), sequencing	17
MabrpoR	5′-AGCCGATCAGACCGATGTT-3′ (positions 2559–2541)[b]		
ITSF	5′-TTGTACACACCGCCCGTC-3′	Mycobacterial 16S-23S ITS region, PCR (ca. 340 bp), sequencing	23
ITSR	5′-TCTCGATGCCAAGGCATCCACC-3′		

[a] Nucleotide positions were assigned using the *Escherichia coli* 16S rRNA gene sequence as a reference.
[b] Primer design and nucleotide positions were based on the *M. tuberculosis rpoB* gene sequence (GenBank/EMBL/DDBJ accession no. L27989).

fication of mycobacterial strains. However, the reference panel for the DDH Mycobacteria kit consists of only the 18 most common strains of mycobacteria. Although the DDH test is able to clearly differentiate *M. chelonae* from the rest of the *M. chelonae-M. abscessus* group, *M. abscessus* subsp. *massiliense* and *M. abscessus* subsp. *bolletii* are not included in the panel (19). In fact, isolates from different subpopulations of patients were all identified as *M. abscessus* by the DDH assay. However, these isolates appeared to have different responses to several antimycobacterial drugs (20). These observations led us to develop a simple genotyping test to discriminate *M. abscessus* subsp. *massiliense* from *M. abscessus* using the whole-genome data of *M. abscessus* subsp. *massiliense* as a reference sequence.

MATERIALS AND METHODS

Bacterial strains. An environmental isolate (strain LRC AbsB-1) and 117 clinical isolates were obtained for differential diagnosis from hospitals in Japan (see the Appendix for the list of the hospitals). Of these, 109 strains were isolated from sputum samples and 8 were obtained from skin lesions (see Table S1 in the supplemental material). All of the isolates had been classified as *M. abscessus* based on the results of DDH analysis (DDH Mycobacteria kit; Kyokuto Pharmaceutical Industrial, Tokyo, Japan). This kit contains 18 strains of mycobacteria on the reference panel, which includes *M. abscessus* but not *M. abscessus* subsp. *massiliense* or *M. abscessus* subsp. *bolletii* (19).

Reference strains of the rapidly growing mycobacteria *M. abscessus* subsp. *massiliense* JCM 15300^T, *M. chelonae* JCM 6388^T, *M. abscessus* subsp. *bolletii* JCM 15297^T, and *M. abscessus* subsp. *abscessus* JCM 13569^T (ATCC 19977) were obtained from the Japan Collection of Microorganisms of the Riken Bio-Resource Center (BRC-JCM; Ibaraki, Japan). All bacterial strains were subcultured on 2% Ogawa egg slants or 7H11 agar plates.

Following development of the multiplex PCR assay, several laboratory and clinical isolates that had been classified using DDH assays and/or sequencing were applied to this assay. They included isolates of *M. avium* complex, *M. fortuitum*, *M. gordonae*, *M. kansasii*, *M. lentiflavum*, *M. peregrinum*, *M. shimoidei*, *M. szulgai*, *M. triplex*, *M. tuberculosis*, and *M. xenopi*.

DNA extraction. DNA extraction was performed as described previously (17). In brief, a loopful of bacilli was suspended in 400 μl sterilized phosphate-buffered saline supplemented with 0.05% Tween 80 and stored at −80°C until the extraction was performed. A frozen sample was crushed with zirconia beads (2 mm in diameter) in a bead-beating instrument. Total genomic DNA was purified from the crushed suspension using a High Pure PCR template preparation kit according to the manufacturer's instructions (Roche Diagnostics) and stored at −20°C.

Sequence analysis. The sequences of the clinical and environmental isolates, which had been preliminarily identified as *M. abscessus* with the DDH kit, were compared to those of the *M. abscessus* subsp. *massiliense* JCM 15300^T, *M. abscessus* subsp. *bolletii* JCM 15297^T, *M. chelonae* JCM 6388^T, and *M. abscessus* subsp. *abscessus* JCM 13569^T reference strains. The sequences of the majority of the 16S rRNA gene, partial *hsp65* and *rpoB* genes, and the internal transcribed spacer (ITS) region between the 16S and 23S rRNA genes were amplified using AmpliTaq Gold DNA polymerase (Applied Biosystems, Foster City, CA) with the primers listed in Table 1. Both strands were sequenced with BigDye Terminator cycle sequencing kit ver. 3.1 (Applied Biosystems) and run on an ABI Prism 3130 Genetic Analyzer (Applied Biosystems). Analyses were performed after removing the primers from the sequences (24).

Short-read DNA sequencing using Illumina Genome Analyzer II. A cDNA library of *M. abscessus* subsp. *massiliense* JCM 15300^T, containing fragments of approximately 500 bp in length, was prepared using a genomic DNA Sample Prep kit (Illumina, San Diego, CA). DNA clusters were generated on a slide using a Cluster Generation kit (ver. 2) on an Illumina Cluster Station (Illumina), according to the manufacturer's instructions. All sequencing runs for 83-mers were performed using Illumina Genome Analyzer II (GA II) and an Illumina sequencing kit (ver. 3). Fluorescent images were analyzed using Illumina base-calling pipeline 1.4.0 to obtain FASTQ-formatted sequence data.

***De novo* assembly of short DNA reads.** Prior to *de novo* assembly, reads were divided into 40-, 50-, 60-, or 70-mers from the 5′ end of 83-mer reads followed by nucleotide trimming based on the *phred* quality value (cutoff of 14) using the Euler-SR *qualitytrimmer* command (25). These trimmed sequences were then assembled using Euler-SR v1.0 (25) with the default parameters (vertex size, 25).

Genome scaffold analysis using reference sequences. Reference sequence-assisted gap closing was performed with OSLay v1.0 software (26) using the *Mycobacterium abscessus* ATCC 19977 chromosome DNA sequence as a reference genome (GenBank accession no. NC_010397). Homologous regions between the *de novo* assembly of short reads and ATCC 19977 chromosome DNA were identified by BLASTN searches with 1E-10 as a cutoff value (setting parameters, -m 8 -e 1E-10). Predicted supercontigs (an ordered and oriented set of contigs that contained gaps) were visualized by OSLay (26). Tentative scaffolds of *M. abscessus* subsp. *massiliense* chromosomal DNA sequence were obtained in the same manner as the supercontigs. Pairwise alignment between those genome sequences was performed using a BLASTN homology search (27) followed by visualization of the aligned images with the Artemis Comparison Tool (ACT) (28).

Downloaded from http://jcm.asm.org/ on December 20, 2013 by NATL INST OF INFECTIOUS DISEAS

TABLE 2 List of DNA sequence accession numbers (AB548592 to AB548611)

Strain	16S rRNA (1,468 bp)	*hsp65* (401 bp)	*rpoB* (409 bp)	ITS (298 bp)
M. abscessus subsp. *massiliense* JCM 15300^T	AB548602	AB548601	AB548600	AB548603
M. abscessus subsp. *bolletii* JCM 15297^T	AB548606	AB548605	AB548604	AB548607
M. abscessus subsp. *abscessus* JCM 13569^T	AB548599	AB548598	AB548597	AB548596
M. abscessus subsp. *massiliense* strain A1	AB548592	AB548593	AB548594	AB548595
M. chelonae JCM 6388^T	AB548610	AB548609	AB548608	AB548611

PCR assays. Single-PCR and multiplex PCR assays differentiating *M. abscessus* subsp. *abscessus* and *M. abscessus* subsp. *massiliense* were conducted with the listed primers (see Table 4). In brief, 50 μl of a mixture containing 50% AmpliTaq Gold 360 Master Mix (Applied Biosystems), 2% GC enhancer, 0.5 μM (each) primer, and 0.1 μg template DNA was used for PCR with a single set of primers. Amplification was performed in the Mastercycler gradient (Eppendorf) using 95°C for 10 min; 30 cycles of 95°C for 1 min, 55°C for 1 min, and 72°C for 1 min; and a final extension at 72°C for 7 min. The PCR products were separated by 2% agarose gel electrophoresis and stained with ethidium bromide.

Nucleotide sequence accession numbers. The DNA sequences of the 16S rRNA (1,468-bp), *hsp65* (401-bp), *rpoB* (409-bp), and ITS (298-bp) fragments from the reference strains (type strains of *M. abscessus* subsp. *massiliense* JCM 15300^T, *M. chelonae* JCM 6388^T, *M. abscessus* subsp. *bolletii* JCM 15297^T, *M. abscessus* subsp. *abscessus* JCM 13569^T, and *M. abscessus* subsp. *massiliense* cutaneous isolate strain A1) were deposited into the International Nucleotide Sequence Databases (INSD) through the DNA Databank of Japan (DDBJ) under accession numbers AB548592 to AB548611 (see Table 2). The draft genome sequences of *M. abscessus* subsp. *massiliense* were deposited under accession numbers BAOM01000001 to BAOM01000060.

RESULTS

Multilocus sequence analysis. Nucleotide sequence analysis was performed with the isolates and reference strains (*M. abscessus* subsp. *abscessus*, *M. abscessus* subsp. *massiliense*, *M. abscessus* subsp. *bolletii*, and *M. chelonae*). The sequences of the 1,468-bp fragment of the 16S rRNA genes of the 118 isolates and the reference strains were almost identical, with only 1-bp mismatches or no mismatches with *M. abscessus* subsp. *abscessus*, *M. abscessus* subsp. *massiliense*, and *M. abscessus* subsp. *bolletii* found at nucleotide position 1007 or 1008 or 1407 or 1408 and additional 3-bp mismatches with *M. chelonae* at nucleotide positions 999, 1039, and 1265 (17). However, differences were observed with the sequences of *hsp65*, *rpoB*, and the ITS region (Table 3). There were two distinct groups. The strains in the first group either had the same *hsp65*/*rpoB*/ITS sequence as the *M. abscessus* subsp. *abscessus* type strain (type 1) or had a 1- or 2-bp difference in *hsp65* and/or the ITS region (type 1a or type 1b). In this group, 58.5% of the strains were classified as *M. abscessus* subsp. *abscessus*, in accordance with the DDH results. The strains in the second group had the same *hsp65*/*rpoB*/ITS sequence as the *M. abscessus* subsp. *massiliense* type strain, with the exception of one base in the ITS region (type 2) or one or two or no base pair differences in the ITS region and/or *rpoB* (type 2a, type 2b, type 2c, and type 2d). In this group, 36.4% of the strains classified as *M. abscessus* by DDH were actually *M. abscessus* subsp. *massiliense*. The strains in the third group, with only 3 isolates included, had the same *hsp65*/*rpoB*/ITS sequence as the *M. abscessus* subsp. *bolletii* type strain, with the exception of 1-bp differences in *rpoB* (type 3a) and/or the ITS region and/or *hsp65* (type 3b and type 3c). In this group, 2.5% of the strains classified as *M. abscessus* by DDH were actually *M. abscessus* subsp. *bolletii*. The remaining three clinical isolates could not be identified by the sequences, because they had discordant sequencing results. The sequences of the *hsp65* genes and ITS regions of the two isolates were identical to those of *M. abscessus* subsp. *abscessus*; however, they carried the *rpoB* sequence of *M. abscessus* subsp. *bolletii* with the 1-bp mismatch (DS type 4). The third isolate had the *M. abscessus* subsp. *massiliense hsp65* and ITS region sequences and the *rpoB* sequence of *M. abscessus* subsp. *abscessus* (DS type 5). An examination of the data from combinations of multilocus sequence analyses can be used to clearly discriminate *M. abscessus* subsp. *abscessus*, *M. abscessus* subsp. *massiliense*, and *M. abscessus* subsp. *bolletii* with 97.5% accuracy.

Whole-genome sequence analysis and primer design. The whole-genome sequence of the *M. abscessus* subsp. *massiliense* type strain was compared with that of the *M. abscessus* subsp. *abscessus* type strain (GenBank accession no. NC_010397) using the ACT to visualize pairwise alignments between the sequences. At least eight notable regions, containing 50- to 800-bp differences, were identified as candidates for PCR targets (i.e., 50- to 800-bp insertions or deletions in *M. abscessus* subsp. *massiliense* compared to *M. abscessus* subsp. *abscessus*). Figure S1 in the supplemental material shows a representative region, which had a 494-bp insertion in *M. abscessus* subsp. *massiliense* at position 3694233 of *M. abscessus* subsp. *abscessus*. The eight regions were labeled MAB_0022c, MAB_0104c, MAB_0357c, MAB_1112c, MAB_1176c, MAB_2847c, MAB_3644, and MAB_4614 with reference to the locations of the open reading frames (ORFs). Regions around MAB_0022c, MAB_0104c, MAB_3644, and MAB_4614 were associated with coding sequences, whereas MAB_0357, MAB_1112c, MAB_1176, and MAB_2847 were associated with noncoding sequences. Eight primer sets were designed using locations in the borders of regions that would sharply differentiate *M. abscessus* subsp. *abscessus* and *M. abscessus* subsp. *massiliense* based on the sizes of their PCR amplicons (Table 4). Single-PCR tests were performed to cull the two best primer sets. The following check points were used as selection criteria. (i) Were the isolates amplified? (ii) Were the amplicons clear single bands? (iii) Were the amplicons the correct size? (iv) Were the PCR results discriminating *M. abscessus* subsp. *abscessus* and *M. abscessus* subsp. *massiliense* consistent with the multilocus sequence analysis? All clinical isolates were used in the single-PCR tests; however, tests were terminated when check point 1, 2, or 3 was negative, with the first 20 strains selected. Figure S2 in the supplemental material shows single-PCR results targeting MAB_1176c as representative. As shown in that figure, PCR of all *M. abscessus* subsp. *abscessus* strains produced an amplicon of the expected size, ca. 210 bp. Four clinical *M. abscessus* subsp. *massiliense* strains and the *M. abscessus* subsp. *massiliense* type strain produced an amplicon of ca. 860 bp. However, 8 clinical strains produced an unexpected size of ca. 400 bp. These results suggested that the MAB 1176c primer sets were not suitable for PCR, since the insertion sequence in the *M. abscessus* subsp. *massiliense* clinical strains was not conserved as a uniformly sized sequence of ca. 860 bp. Single-PCR results are shown in Table S2 in the supplemental material. Amplification using MAB 3644, MAB 0022c, and MAB 1112c primer sets produced amplicons of

Downloaded from http://jcm.asm.org/ on December 20, 2013 by NATL INST OF INFECTIOUS DISEAS

TABLE 3 The sequential differences in clinical isolates in *M. abscessus sensu lato*

Group	No. of tested strains	Predicted DDH result	Nucleotide sequence position[a]																																
			hsp65[b]							*rpoB*[c]																ITS region									
			115	118	127	187	190	229	340	10	31	79	88	124	127	136	193	202	277	283	316	343	376	379	25	45	48	60	101–103[d]	180	276					
M. abscessus subsp. *abscessus*[T]	1	*M. abscessus*	T	T	C	C	C	G	C	T	T	C	T	G	C	T	C	C	C	C	T	C	C	C	T	A	C	A	C-G	C	G					
Type 1	61	*M. abscessus*	T	T	C	C	C	G	C	T	T	C	T	G	C	T	C	C	C	C	T	C	C	C	T	A	C	A	C-G	C	G					
Type 1a	6	*M. abscessus*	T	T	C	C	C	G	C	T	T	C	T	G	C	T	C	C	C	C	T	C	C	C	T	A	T	A	C-G	C	G					
Type 1b	2	*M. abscessus*	T	T	C	C	C	G	T	T	T	C	T	G	C	T	C	C	C	C	T	C	C	C	T	A	T	A	C-G	C	G					
M. abscessus subsp. *massiliense*[T]	1	*M. abscessus*	G	C	T	C	T	G	T	C	C	C	C	A	T	C	C	G	T	C	C	T	T	T	T	A	C	G	CCG	C	A					
Type 2	29	*M. abscessus*	G	C	T	C	T	G	T	C	C	C	C	A	T	C	C	G	T	C	C	T	T	T	T	A	C	G	CCG	T	A					
Type 2a	10	*M. abscessus*	G	C	T	C	T	G	T	C	C	C	C	A	T	C	C	G	T	C	C	T	T	T	C	A	C	G	CCG	T	A					
Type 2b	2	*M. abscessus*	G	C	T	C	T	G	T	C	C	C	C	A	T	C	C	G	T	C	T	T	T	T	T	A	C	G	CCG	C	A					
Type 2c	1	*M. abscessus*	G	C	T	C	T	G	T	C	C	C	C	A	T	C	C	G	T	C	T	T	T	T	C	A	C	G	CCG	C	A					
Type 2d	1	*M. abscessus*	G	C	T	C	T	G	T	C	C	C	C	A	T	C	C	G	T	C	C	T	T	T	T	A	C	G	CCG	C	A					
M. abscessus subsp. *bolletii*[T]	1	*M. abscessus*	G	C	T	T	T	C	C	G	T	T	C	A	T	C	T	T	T	T	T	T	T	T	T	A	C	A	C-G	C	G					
Type 3a	1	*M. abscessus*	G	C	T	T	T	C	C	G	T	T	C	A	T	C	T	C	T	T	T	T	T	T	T	A	C	A	C-G	C	G					
Type 3b	1	*M. abscessus*	G	C	T	T	T	C	C	G	T	T	C	A	T	C	T	C	T	T	T	T	T	T	T	G	C	A	C-G	C	G					
Type 3c	1	*M. abscessus*	G	C	T	C	T	C	C	G	T	T	C	A	T	C	T	T	T	T	T	T	T	T	T	G	C	A	C-G	C	G					
DS[e] type 4	2	*M. abscessus*	T	T	C	C	C	G	C	G	T	T	C	A	T	C	T	C	T	T	T	T	T	T	T	A	C	A	C-G	C	G					
DS type 5	1	*M. abscessus*	G	C	T	C	T	G	T	T	T	C	T	G	C	T	C	C	C	C	T	C	C	C	T	A	C	G	CCG	C	A					

[a] Bold letters indicate nucleotides different from those of the type strains.

[b] Nucleotide positions were based on the *M. abscessus* subsp. *massiliense* sequence of the partial *hsp65* gene (accession no. AB548601).

[c] Nucleotide positions were based on the *M. abscessus* subsp. *massiliense* sequence of the partial *rpoB* gene (accession no. AB548600).

[d] Base deficient.

[e] Isolate showing discordant sequencing results.

Downloaded from http://jcm.asm.org/ on December 20, 2013 by NATL INST OF INFECTIOUS DISEAS

TABLE 4 Primers to discriminate reference strains of *M. abscessus* subsp. *abscessus* and *M. abscessus* subsp. *massiliense*

Primer	Sequence (locations)[a]	Amplified fragment size (ca. bp) of *M. abscessus* subsp. *abscessus*/*M. abscessus* subsp. *massiliense*[b]
MAB 0022cF	5′-TTCGATTCTCCTAGGCTCCA-3′ (22165–22184)	220/270
MAB 0022cR	5′-GGCGTACATGACCGCATACT-3′ (22386–22367)	
MAB 0104cF	5′-GGTGACTGAACTCCACGAAGA-3′ (105362–105382)	590/160
MAB 0104cR	5′-CGATATCGTGAGCCATCCTC-3′ (105948–105929)	
MAB 0357cF	5′-GGTAGCTCTTCCAGCCGAAT-3′ (354468–354487)	900/300
MAB 0357cR	5′-CAGCACGCA AAGGTACGAC-3′ (355376–355358)	
MAB 1112cF	5′-CCAAAACCGTTGAGCGTTAT-3′ (1125571–1125590)	200/1,020
MAB 1112cR	5′-ATCATGAACCGCAAGTACCG-3′ (1125776–1125757)	
MAB 1176cF	5′-CACACCACGTGTCCTACAGC-3′ (1193378–1193397)	210/860
MAB 1176cR	5′-AGTCCATCGAACGAACTTGG-3′ (1193594–1193575)	
MAB 2847cF	5′-CCCACAAATTTCGTAAGACCA-3′ (2896496–2896516)	130/200
MAB 2847cR	5′-ACCCAGGTGGAACTCTTCAC-3′ (2896628–2896609)	
MAB 3644F	5′-GTCACCGCAGAAATCGAGTC-3′ (3694129–3694148)	200/700
MAB 3644R	5′-GGGGTGGTTGACGTGTTC-3′ (3694310–3694293)	
MAB 3644 (Rev2R)[c]	5′-CGAGGTCAAGTGGCTTCTTT-3′ (3694262–3694243)	150/650
MAB 4614F	5′-CCTTCACCCTTCCGTTCAT-3′ (4698970–4698988)	215/535
MAB 4614R	5′-GTTGGGACTGCAGGTATTGC-3′ (4699184–4699165)	

[a] Nucleotide positions were based on the complete sequence of the *M. abscessus* subsp. *abscessus* chromosome (accession no. CU458896) as a reference.
[b] Fragment sizes were predicted from the results of sequencing of the draft genome of *M. abscessus* subsp. *massiliense* (accession no. BAOM01000001 to BAOM01000060).
[c] MAB 3644 (Rev2R) was used only in the multiplex PCR.

the proper size, although some of the clinical strains displayed contrasting results. We concluded that the combined targeting of MAB_0357c and MAB_3644 would produce the best results (Fig. 1 and 2). These regions generated amplicons of the correct size, delivered results that were consistent with those of multilocus sequence analysis, and provided an easy visual means to distinguish between *M. abscessus* subsp. *abscessus* and *M. abscessus* subsp. *massiliense*.

Discriminatory multiplex PCR assay. Based on the results of single PCR, we performed amplifications using the clinical strains. All of the clinical isolates that were initially identified as *M. abscessus* by DDH could be resolved as *M. abscessus* subsp. *abscessus* or *M. abscessus* subsp. *massiliense* using both sets of primer pairs MAB 0357c and MAB 3644. However, the amplification results were not always clear enough: it has been speculated that *Taq* polymerase is heavily utilized to amplify shorter bands, leaving many weak longer bands (data not shown). For more clearly balanced multiplex amplification, MAB 3644R was replaced with MAB 3644 (Rev2R) (Fig. 3). Using MAB 0357c and MAB 3644 (Rev2R) allowed a clear separation of *M. abscessus* subsp. *abscessus* isolates from *M. abscessus* subsp. *massiliense* isolates (Table 5; see also Table S1 in the supplemental material). Multiplex PCR results from the three type strains and 118 clinical isolates are shown in Table S1. A total of 70 *M. abscessus* subsp. *abscessus* isolates showed the same multiplex PCR pattern (ca. 900 bp and ca. 150 bp), and 44 *M. abscessus* subsp. *massiliense* isolates showed ca. 300 bp and ca. 650 bp. However, the results for 4 isolates of *M. abscessus* subsp. *bolletii* were not converged. One of the clinical isolates (type 3a) and the type strain showed an amplification pattern that was identical to that of *M. abscessus* subsp. *abscessus* (ca. 900 bp and ca. 150 bp). The two other clinical isolates (types 3b and 3c) showed different patterns, ca. 150 bp and ca. 300 bp and a weak pattern of ca. 300 bp and ca. 650 bp, respectively. The discordant results from two type 4 isolates were identical to those obtained for *M. abscessus* subsp. *bolletii* type 3b, showing a multiplex PCR pattern of ca. 150 bp and ca. 300 bp. The pattern determined for the remaining type 5 discordant isolate was identical to that of *M. abscessus* subsp. *massiliense*, ca. 300 bp and ca. 650 bp. All other mycobacterial isolates prepared as negative controls were negative in this multiplex PCR assay. The only exception was the *M. che-*

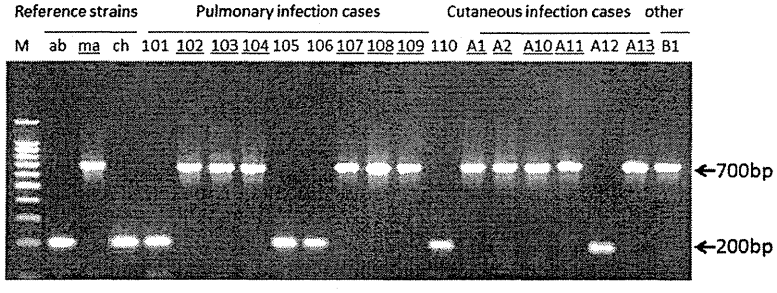

FIG 1 Representative single-PCR results for the reference strains and clinical isolates amplified with primer pair MAb 3644F and MAb 3644R. The numbers are the strain numbers of the clinical isolates. Underlining indicates that *M. abscessus* subsp. *massiliense* (ma) was classified after the multilocus genotyping assay shown in Table 3. The *M. abscessus* subsp. *massiliense* PCR product was fully amplified to 700 bp. However, the *M. abscessus* subsp. *abscessus* (ab) and *M. chelonae* (ch) amplicons amplified to 200 bp in size.

Downloaded from http://jcm.asm.org/ on December 20, 2013 by NATL INST OF INFECTIOUS DISEAS

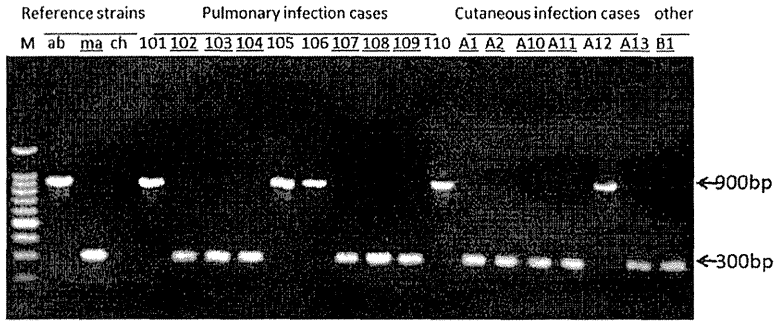

FIG 2 Representative single-PCR results for the reference strains and clinical isolates amplified with primer pair MAb 0357cF and MAb 0357cR. The numbers are the strain numbers of the clinical isolates. Underlining indicates that *M. abscessus* subsp. *massiliense* (ma) was classified after the multilocus genotyping assay shown in Table 3. The *M. abscessus* subsp. *abscessus* (ab) PCR product was fully amplified to 900 bp in size. However, the *M. abscessus* subsp. *massiliense* amplicon was 300 bp in size, while *M. chelonae* (ch) did not amplify.

lonae type strain, which showed a single weak band of ca. 200 bp (Fig. 3).

DISCUSSION

We have developed a simple, cost-effective discriminative multiplex PCR to differentiate *M. abscessus* subsp. *massiliense* from *M. abscessus* subsp. *abscessus* and from other RGM. The multiplex PCR expanded upon the results of two sets of discriminative single PCRs to concurrently amplify *M. abscessus* subsp. *abscessus* and *M. abscessus* subsp. *massiliense* and distinguish them based upon differences in amplicon size. In order to achieve the different amplifications in length, clear insertion or deletion regions between *M. abscessus* subsp. *massiliense* and *M. abscessus* subsp. *abscessus* whole-genome sequences were selected for the single-PCR targets using the Artemis Comparison Tool. The combination of MAB 0357c and MAB 3644 (Rev2R) for targeted PCR mainly leads to two distinct visual patterns that are easily read by novice PCR technologists. Previously, clinicians identified all isolates as *M. abscessus* because the use of the DDH assay was very common in Japan. The isolates were also grouped together because of their colony morphologies, growth profiles, and biochemical characteristics. Even the majority of the sequences of their 16S rRNA genes are the same. However, clinicians began to suspect that different strains were present because there were significantly different clinical outcomes and drug susceptibility groups among these isolates. For example, *M. abscessus* subsp. *massiliense* is more susceptible to azithromycin than *M. abscessus* subsp. *abscessus* but not to clofazimine, meropenem, and panipenem (17). Thus, correct and rapid species identification could facilitate the clinical treatment of mycobacterial infections (7). Two distinct genotypes were eventually observed in isolates identified as *M. abscessus* by the DDH mycobacterial assays (17). These two groups can be separated by a combinational genotypic analysis of the sequences of the ITS region and *hsp65* and *rpoB* genes. Similarly, in other reports of multilocus sequencing analysis performed with *hsp65*, *rpoB*, and *secA1* (4) or with eight housekeeping genes (29), *M. abscessus* subsp. *abscessus*, *M. abscessus* subsp. *massiliense*, and *M. abscessus* subsp. *bolletii* are clearly differentiated. But this methodology is not practical due to the cost and effort involved. There have been other PCR-based methods, such as erythromycin ribosome methyltransferase (*erm*) PCR (8) and variable-number tandem-repeat (VNTR) analysis (30). *erm* PCR is also a very simple and accurate method but, having only one target, can easily lead to false-negative results. The VNTR method is not easy for nonexperts.

A study in South Korea found that 51% of the *M. chelonae-M. abscessus* group is comprised of *M. abscessus* subsp. *abscessus* and 47% is *M. abscessus* subsp. *massiliense* (11). A typing study of *M. abscessus* subsp. *abscessus*, *M. abscessus* subsp. *massiliense*, and *M. abscessus* subsp. *bolletii* performed in the United States showed that 64% of the isolates were *M. abscessus* subsp. *abscessus* and 28% were *M. abscessus* subsp. *massiliense* (4). In France, 60% of the isolates belonged to *M. abscessus* subsp. *abscessus* and 22% to *M.*

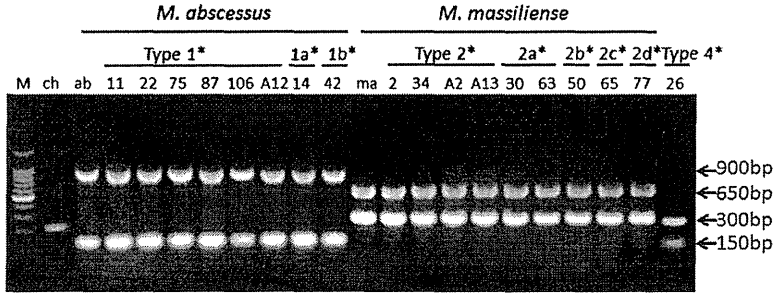

FIG 3 Representative multiplex PCR results for the reference strains and clinical isolates amplified with primer pair MAB 3644F and MAB 3644 (Rev2R) and primer pair MAB 0357cF and MAB 0357cR. *, types 1, 1a, and 1b, types 2, 2a, 2b, 2c, and 2d, and type 4 are the groupings of the clinical isolates based on their sequences (Table 3). The numerals below the groupings are the strain numbers of the clinical isolates.

Downloaded from http://jcm.asm.org/ on December 20, 2013 by NATL INST OF INFECTIOUS DISEAS

TABLE 5 PCR results compared with other genetic classifications

Group	No. of tested strains	Predicted DDH result	Classification by *hsp65*/*rpoB*/ITS sequences[a]	PCR result(s) (ca. bp) with primer pair(s): MAB 3644F + MAB 3644R	MAB 0357cF + MAB 0357cR	MAB 3644F + MAB 3644 (Rev2R), MAB 0357cF + MAB 0357cR
M. abscessus subsp. *abscessus*^{T}	1	*M. abscessus*	*M. abscessus* subsp. *abscessus*	200	900	900, 150
Type 1	61	*M. abscessus*	*M. abscessus* subsp. *abscessus*	200	900	900, 150
Type 1a	6	*M. abscessus*	*M. abscessus* subsp. *abscessus*	200	900	900, 150
Type 1b	2	*M. abscessus*	*M. abscessus* subsp. *abscessus*	200	900	900, 150
M. abscessus subsp. *massiliense*^{T}	1	*M. abscessus*	*M. abscessus* subsp. *massiliense*	700	300	300, 650
Type 2	29	*M. abscessus*	*M. abscessus* subsp. *massiliense*	700	300	300, 650
Type 2a	10	*M. abscessus*	*M. abscessus* subsp. *massiliense*	700	300	300, 650
Type 2b	2	*M. abscessus*	*M. abscessus* subsp. *massiliense*	700	300	300, 650
Type 2c	1	*M. abscessus*	*M. abscessus* subsp. *massiliense*	700	300	300, 650
Type 2d	1	*M. abscessus*	*M. abscessus* subsp. *massiliense*	700	300	300, 650
M. abscessus subsp. *bolletii*^{T}	1	*M. abscessus*	*M. abscessus* subsp. *bolletii*	200	900	900, 150
Type 3a	1	*M. abscessus*	*M. abscessus* subsp. *bolletii*	200	900	900, 150
Type 3b	1	*M. abscessus*	*M. abscessus* subsp. *bolletii*	200	300	300, 150
Type 3c	1	*M. abscessus*	*M. abscessus* subsp. *bolletii*	700	300[b]	300[b], 650
DS[c] type 4	2	*M. abscessus*	*M. abscessus* subsp. *abscessus*-*M. abscessus* subsp. *bolletii*[d]	200	300	300, 150
DS type 5	1	*M. abscessus*	*M. abscessus* subsp. *massiliense*-*M. abscessus* subsp. *abscessus*[e]	700	300	300, 650

[a] Classifications were determined on the basis of the overall results of sequencing of *hsp65*, *rpoB*, and the ITS region (Table 3).
[b] Weak band.
[c] Isolate showing discordant sequencing results.
[d] Isolate showing *M. abscessus* subsp. *abscessus hsp65* and *M. abscessus* subsp. *bolletii rpoB* sequences.
[e] Isolate showing *M. abscessus* subsp. *massiliense hsp65* and ITS region and *M. abscessus* subsp. *abscessus rpoB* sequences.

abscessus subsp. *massiliense* (13), while in Japan, 71% belonged to *M. abscessus* subsp. *abscessus* and 26% to *M. abscessus* subsp. *massiliense* (20). In pulmonary patients in the Netherlands diagnosed with infections by strains from the *M. chelonae-M. abscessus* group, 50% of the isolates were identified as *M. abscessus* subsp. *abscessus* and 29% as *M. abscessus* subsp. *massiliense* (31). In accordance with the recent study in Japan mentioned above (20), we can estimate that more than 30% of patients diagnosed with *M. abscessus* subsp. *abscessus* should differentiate as *M. abscessus* subsp. *massiliense* patients. Some isolates might be colonizers whereas others might have appeared after prolonged treatment of infections by other nontuberculous mycobacteria. Therefore, we are currently collecting patient treatment data from the hospitals that participated in this study and are analyzing the relationship between clinical isolates and treatment history.

Three clinical isolates were not identified to the species level by multilocus sequence analysis. They are discordant isolates that were previously reported by Zelazny et al. (4) and Macheras et al. (29). The sequences of the *hsp65* genes and ITS regions of the two isolates were identical to those of *M. abscessus* subsp. *abscessus*; however, they carried the *rpoB* sequence of *M. abscessus* subsp. *bolletii* with the 1-bp mismatch (DS type 4). Both strains produced multiplex PCR amplicons of ca. 300 bp and ca. 150 bp, like those of *M. abscessus* subsp. *bolletii* type 3b (see Table S1 in the supplemental material). The third isolate which had the *M. abscessus* subsp. *massiliense hsp65* and ITS regions and the *rpoB* sequence of *M. abscessus* subsp. *abscessus* (DS type 5) had the multiplex PCR pattern of *M. abscessus* subsp. *massiliense* (ca. 300 bp and ca. 650 bp). Although those strains are very rare, they are interesting in that they suggest the occurrence of horizontal gene transfer. Such discordant isolates would produce different amplicons (ca. 300 bp and ca. 150 bp) from *M. abscessus* subsp. *abscessus* and *M. abscessus* subsp. *massiliense* (Table 5).

In the case of RGM infection, we propose the use of this multiplex PCR assay as a first step, because it can be used by inexperienced technicians to identify *M. abscessus* subsp. *abscessus* and *M. abscessus* subsp. *massiliense* quickly and accurately. In addition, there is no need to prepare purified DNA; the supernatant from a boiled bacterial suspension can be used (data not shown). The resulting band patterns of 900 bp and 150 bp and of 300 bp and 650 bp imply the identification of *M. abscessus* subsp. *abscessus* and *M. abscessus* subsp. *massiliense* with 97.2% and 95.7% accuracy. Another rare pattern, 300 bp and 150 bp, implies identification of a discordant strain with 66.7% accuracy. Although this multiplex PCR method conduces to reasonably accurate discrimination, it cannot be used to differentiate *M. abscessus* subsp. *bolletii* from *M. abscessus* subsp. *abscessus* or *M. abscessus* subsp. *massiliense*, because all three clinical isolates of *M. abscessus* subsp. *bolletii* showed different multiplex PCR patterns in this study (Table 5).

As a result of this study, we have developed a simple, rapid

Downloaded from http://jcm.asm.org/ on December 20, 2013 by NATL INST OF INFECTIOUS DISEAS

methodology to distinguish between *M. abscessus* subsp. *abscessus* and *M. abscessus* subsp. *massiliense*. This approach, which spans whole-genome sequencing and clinical diagnosis, will facilitate the acquisition of more precise information about bacterial genomes, aid in the choice of more-relevant therapies, and promote the advancement of novel discrimination and differential diagnostic assays.

APPENDIX

The clinical isolates used in this study were sent from the hospitals and universities described below. Specimens were originally collected for disease diagnosis. The portion remaining after diagnosis was used for this study. We appreciate the work of all of the clinicians in the following institutions who took care of patients infected with these mycobacteria: Hokkaido Social Insurance Hospital, Japan Anti-Tuberculosis Association (JATA) Fukujuji Hospital, Saitama Medical University, National Hospital Organization (NHO) Tokyo National Hospital, Showa University Fujigaoka Hospital, National Defense Medical College Hospital, Kyorin University Hospital, NHO Minami-Kyoto Hospital, Kyoto Prefectural University of Medicine, JATA Osaka Hospital, NHO Kinki-Chuo Chest Medical Center, NHO Matsue Medical Center, NHO Higashihiroshima Medical Center, Kawasaki Medical School, Kyosai-Yoshijima Hospital, and NHO Omuta Hospital.

ACKNOWLEDGMENTS

We appreciate Ms Katsue Ishii (Fukujuji Hospital) for preparing negative control of clinical isolates.

This work was supported in part by a Grant-in-Aid for Research on Emerging and Re-emerging Infectious Diseases from the Ministry of Health, Labor, and Welfare of Japan for Y.H., M.M., and N.I. and by a Grant-in-Aid for Scientific Research (C) from the Ministry of Education, Culture, Sports, Science and Technology of Japan for Y.H. and by a Grant-in-Aid for Scientific Research (C) from the Japan Society for the Promotion of Science for K.N.

REFERENCES

1. Viana-Niero C, Lima KV, Lopes ML, Rabello MC, Marsola LR, Brilhante VC, Durham AM, Leão SC. 2008. Molecular characterization of *Mycobacterium massiliense* and *Mycobacterium bolletii* in isolates collected from outbreaks of infections after laparoscopic surgeries and cosmetic procedures. J. Clin. Microbiol. 46:850–855. http://dx.doi.org/10.1128/JCM.02052-07.
2. Simmon KE, Pounder JI, Greene JN, Walsh F, Anderson CM, Cohen S, Petti CA. 2007. Identification of an emerging pathogen, Mycobacterium massiliense, by *rpoB* sequencing of clinical isolates collected in the United States. J. Clin. Microbiol. 45:1978–1980. http://dx.doi.org/10.1128/JCM.00563-07.
3. Cardoso AM, Martins de Sousa E, Viana-Niero C, Bonfim de Bortoli F, Pereira das Neves ZC, Leão SC, Junqueira-Kipnis AP, Kipnis A. 2008. Emergence of nosocomial *Mycobacterium massiliense* infection in Goiás, Brazil. Microbes Infect. 10:1552–1557. http://dx.doi.org/10.1016/j.micinf.2008.09.008.
4. Zelazny AM, Root JM, Shea YR, Colombo RE, Shamputa IC, Stock F, Conlan S, McNulty S, Brown-Elliott BA, Wallace RJ, Jr, Olivier KN, Holland SM, Sampaio EP. 2009. Cohort study of molecular identification and typing of *Mycobacteriumabscessus,Mycobacterium massiliense*, and *Mycobacterium bolletii*. J. Clin. Microbiol. 47:1985–1995. http://dx.doi.org/10.1128/JCM.01688-08.
5. Adékambi T, Reynaud-Gaubert M, Greub G, Gevaudan MJ, La Scola B, Raoult D, Drancourt M. 2004. Amoebal coculture of "*Mycobacterium massiliense*" sp. nov. from the sputum of a patient with hemoptoic pneumonia. J. Clin. Microbiol. 42:5493–5501. http://dx.doi.org/10.1128/JCM.42.12.5493-5501.2004.
6. Adékambi T, Berger P, Raoult D, Drancourt M. 2006. rpoB gene sequence-based characterization of emerging non-tuberculous mycobacteria with descriptions of *Mycobacterium bolletii sp. nov., Mycobacterium phocaicum* sp. nov. and *Mycobacterium aubagnense* sp. nov. Int. J. Syst. Evol. Microbiol. 56(Pt 1):133–143. http://dx.doi.org/10.1099/ijs.0.63969-0.
7. Koh WJ, Jeon K, Lee NY, Kim BJ, Kook YH, Lee SH, Park YK, Kim CK, Shin SJ, Huitt GA, Daley CL, Kwon OJ. 2011. Clinical significance of differentiation of *Mycobacterium massiliense* from *Mycobacterium abscessus*. Am. J. Respir. Crit. Care Med. 183:405–410. http://dx.doi.org/10.1164/rccm.201003-0395OC.
8. Kim HY, Kim BJ, Kook Y, Yun YJ, Shin JH, Kim BJ, Kook YH. 2010. *Mycobacterium massiliense* is differentiated from *Mycobacterium abscessus* and *Mycobacterium bolletii* by erythromycin ribosome methyltransferase gene (erm) and clarithromycin susceptibility patterns. Microbiol. Immunol. 54:347–353. http://dx.doi.org/10.1111/j.1348-0421.2010.00221.x.
9. Leao SC, Tortoli E, Euzéby JP, Garcia MJ. 2011. Proposal that *Mycobacterium massiliense* and *Mycobacterium bolletii* be united and reclassified as *Mycobacterium abscessus* subsp. *bolletii* comb. nov., designation of *Mycobacterium abscessus* subsp. *abscessus* subsp. nov. and emended description of *Mycobacterium abscessus*. Int. J. Syst. Evol. Microbiol. 61(Pt 9):2311–2313. http://dx.doi.org/10.1099/ijs.0.023770-0.
10. Bryant JM, Grogono DM, Greaves D, Foweraker J, Roddick I, Inns T, Reacher M, Haworth CS, Curran MD, Harris SR, Peacock SJ, Parkhill J, Floto RA. 2013. Whole-genome sequencing to identify transmission of *Mycobacterium abscessus* between patients with cystic fibrosis: a retrospective cohort study. Lancet 381:1551–1560. http://dx.doi.org/10.1016/S0140-6736(13)60632-7.
11. Kim HY, Yun YJ, Park CG, Lee DH, Cho YK, Park BJ, Joo SI, Kim EC, Hur YJ, Kim BJ, Kook YH. 2007. Outbreak of *Mycobacterium massiliense* infection associated with intramuscular injections. J. Clin. Microbiol. 45:3127–3130. http://dx.doi.org/10.1128/JCM.00608-07.
12. Tortoli E, Gabini R, Galanti I, Mariottini A. 2008. Lethal *Mycobacterium massiliense* sepsis, Italy. Emerg. Infect. Dis. 14:984–985. http://dx.doi.org/10.3201/eid1406.080194.
13. Roux AL, Catherinot E, Ripoll F, Soismier N, Macheras E, Ravilly S, Bellis G, Vibet MA, Le Roux E, Lemonnier L, Gutierrez C, Vincent V, Fauroux B, Rottman M, Guillemot D, Gaillard JL; Jean-Louis Herrmann for the Group OMA. 2009. Multicenter study of prevalence of nontuberculous mycobacteria in patients with cystic fibrosis in France. J. Clin. Microbiol. 47:4124–4128. http://dx.doi.org/10.1128/JCM.01257-09.
14. Kobashi Y, Mouri K, Obase Y, Miyashita N, Nakanaga K, Oka M. 2011. Pulmonary *Mycobacterium massiliense* disease with septicemia during immunosuppressive treatment. Intern. Med. 50:1069–1073. http://dx.doi.org/10.2169/internalmedicine.50.4733.
15. Hamamoto T, Yuki A, Naoi K, Kawakami S, Banba Y, Yamamura T, Hikota R, Watanabe J, Kimura F, Nakanaga K, Hoshino Y, Ishii N, Shimazaki H, Nakanishi K, Tamai S. 2012. Bacteremia due to *Mycobacterium massilinese* in a patient with chronic myelogenous leukemia: case report. Diagn. Microbiol. Infect. Dis. 74:183–185. http://dx.doi.org/10.1016/j.diagmicrobio.2012.06.009.
16. Otsuki T, Izaki S, Nakanaga K, Hoshino Y, Ishii N, Osamura K. 2012. Cutaneous *Mycobacterium massiliense* infection: a sporadic case in Japan. J. Dermatol. 39:569–572. http://dx.doi.org/10.1111/j.1346-8138.2011.01339.x.
17. Nakanaga K, Hoshino Y, Era Y, Matsumoto K, Kanazawa Y, Tomita A, Furuta M, Washizu M, Makino M, Ishii N. 2011. Multiple cases of cutaneous *Mycobacterium massiliense* infection in a "hot spa" in Japan. J. Clin. Microbiol. 49:613–617. http://dx.doi.org/10.1128/JCM.00817-10.
18. Choi GE, Shin SJ, Won CJ, Min KN, Oh T, Hahn MY, Lee K, Lee SH, Daley CL, Kim S, Jeong BH, Jeon K, Koh WJ. 2012. Macrolide treatment for *Mycobacterium abscessus* and *Mycobacterium massiliense* infection and inducible resistance. Am. J. Respir. Crit. Care Med. 186:917–925. http://dx.doi.org/10.1164/rccm.201111-2005OC.
19. Kusunoki S, Ezaki T, Tamesada M, Hatanaka Y, Asano K, Hashimoto Y, Yabuuchi E. 1991. Application of colorimetric microdilution plate hybridization for rapid genetic identification of 22 *Mycobacterium* species. J. Clin. Microbiol. 29:1596–1603.
20. Harada T, Akiyama Y, Kurashima A, Nagai H, Tsuyuguchi K, Fujii T, Yano S, Shigeto E, Kuraoka T, Kajiki A, Kobashi Y, Kokubu F, Sato A, Yoshida S, Iwamoto T, Saito H. 2012. Clinical and microbiological differences between *Mycobacterium abscessus* and *Mycobacterium massiliense* lung diseases. J. Clin. Microbiol. 50:3556–3561. http://dx.doi.org/10.1128/JCM.01175-12.
21. Springer B, Wu WK, Bodmer T, Haase G, Pfyffer GE, Kroppenstedt RM, Schroder KH, Emler S, Kilburn JO, Kirschner P, Telenti A, Coyle MB, Böttger EC. 1996. Isolation and characterization of a unique group of slowly growing mycobacteria: description of *Mycobacterium lentiflavum* sp. nov. J. Clin. Microbiol. 34:1100–1107.

Downloaded from http://jcm.asm.org/ on December 20, 2013 by NATL INST OF INFECTIOUS DISEAS

22. **Telenti A, Marchesi F, Balz M, Bally F, Böttger EC, Bodmer T.** 1993. Rapid identification of mycobacteria to the species level by polymerase chain reaction and restriction enzyme analysis. J. Clin. Microbiol. 31:175–178.
23. **Roth A, Fischer M, Hamid ME, Michalke S, Ludwig W, Mauch H.** 1998. Differentiation of phylogenetically related slowly growing mycobacteria based on 16S-23S rRNA gene internal transcribed spacer sequences. J. Clin. Microbiol. 36:139–147.
24. **Nakanaga K, Ishii N, Suzuki K, Tanigawa K, Goto M, Okabe T, Imada H, Kodama A, Iwamoto T, Takahashi H, Saito H.** 2007. "*Mycobacterium ulcerans* subsp. *shinshuense*" isolated from a skin ulcer lesion: identification based on 16S rRNA gene sequencing. J. Clin. Microbiol. 45:3840–3843. http://dx.doi.org/10.1128/JCM.01041-07.
25. **Chaisson MJ, Pevzner PA.** 2008. Short read fragment assembly of bacterial genomes. Genome Res. 18:324–330. http://dx.doi.org/10.1101/gr.7088808.
26. **Richter DC, Schuster SC, Huson DH.** 2007. OSLay: optimal syntenic layout of unfinished assemblies. Bioinformatics 23:1573–1579. http://dx.doi.org/10.1093/bioinformatics/btm153.
27. **Altschul SF, Madden TL, Schaffer AA, Zhang J, Zhang Z, Miller W, Lipman DJ.** 1997. Gapped BLAST and PSI-BLAST: a new generation of protein database search programs. Nucleic Acids Res. 25:3389–3402. http://dx.doi.org/10.1093/nar/25.17.3389.
28. **Carver TJ, Rutherford KM, Berriman M, Rajandream MA, Barrell BG, Parkhill J.** 2005. ACT: the Artemis Comparison Tool. Bioinformatics 21:3422–3423. http://dx.doi.org/10.1093/bioinformatics/bti553.
29. **Macheras E, Roux AL, Ripoll F, Sivadon-Tardy V, Gutierrez C, Gaillard JL, Heym B.** 2009. Inaccuracy of single-target sequencing for discriminating species of the *Mycobacterium abscessus* group. J. Clin. Microbiol. 47:2596–2600. http://dx.doi.org/10.1128/JCM.00037-09.
30. **Wong YL, Ong CS, Ngeow YF.** 2012. Molecular typing of *Mycobacterium abscessus* based on tandem-repeat polymorphism. J. Clin. Microbiol. 50:3084–3088. http://dx.doi.org/10.1128/JCM.00753-12.
31. **van Ingen J, de Zwaan R, Dekhuijzen RP, Boeree MJ, van Soolingen D.** 2009. Clinical relevance of *Mycobacterium chelonae-abscessus* group isolation in 95 patients. J. Infect. 59:324–331. http://dx.doi.org/10.1016/j.jinf.2009.08.016.

Downloaded from http://jcm.asm.org/ on December 20, 2013 by NATL INST OF INFECTIOUS DISEAS

CVI
Journals.ASM.org

Efficient Activation of Human T Cells of Both CD4 and CD8 Subsets by Urease-Deficient Recombinant *Mycobacterium bovis* BCG That Produced a Heat Shock Protein 70-*M. tuberculosis*-Derived Major Membrane Protein II Fusion Protein

Tetsu Mukai, Yumiko Tsukamoto, Yumi Maeda, Toshiki Tamura, Masahiko Makino

Department of Mycobacteriology, Leprosy Research Center, National Institute of Infectious Diseases, Tokyo, Japan

For the purpose of obtaining *Mycobacterium bovis* bacillus Calmette-Guérin (BCG) capable of activating human naive T cells, urease-deficient BCG expressing a fusion protein composed of *Mycobacterium tuberculosis*-derived major membrane protein II (MMP-II) and heat shock protein 70 (HSP70) of BCG (BCG-DHTM) was produced. BCG-DHTM secreted the HSP70-MMP-II fusion protein and effectively activated human monocyte-derived dendritic cells (DCs) by inducing phenotypic changes and enhanced cytokine production. BCG-DHTM-infected DCs activated naive T cells of both CD4 and naive CD8 subsets, in an antigen (Ag)-dependent manner. The T cell activation induced by BCG-DHTM was inhibited by the pretreatment of DCs with chloroquine. The naive $CD8^+$ T cell activation was mediated by the transporter associated with antigen presentation (TAP) and the proteosome-dependent cytosolic cross-priming pathway. Memory $CD8^+$ T cells and perforin-producing effector $CD8^+$ T cells were efficiently produced from the naive T cell population by BCG-DHTM stimulation. Single primary infection with BCG-DHTM in C57BL/6 mice efficiently produced T cells responsive to *in vitro* secondary stimulation with HSP70, MMP-II, and *M. tuberculosis*-derived cytosolic protein and inhibited the multiplication of subsequently aerosol-challenged *M. tuberculosis* more efficiently than did vector control BCG. These results indicate that the introduction of MMP-II and HSP70 into urease-deficient BCG may be useful for improving BCG for control of tuberculosis.

Mycobacterium tuberculosis is a causative bacterium of tuberculosis. One-third of the global population is latently infected with *M. tuberculosis*, which is responsible for 1.4 million deaths worldwide each year (1–4). Recently, multidrug-resistant strains of *M. tuberculosis* have emerged and spread worldwide (5), which mandates the development of reliable preventive measures and therapeutic tools. The manifestation of adult lung tuberculosis cannot be prevented by currently used *Mycobacterium bovis* BCG (6); therefore, the development of more-effective single-injection vaccines is strongly desired.

Host defenses against *M. tuberculosis* are conducted largely by type 1 T cells of both CD4 and CD8 subsets (7–9). As one of the most important effector elements, gamma interferon (IFN-γ) is well known (10). IFN-γ can be produced chiefly by $CD4^+$ T cells and $CD8^+$ T cells. $CD8^+$ T cells are also required to differentiate into cytotoxic T lymphocytes capable of killing *M. tuberculosis*-infected macrophages and dendritic cells (DCs) (11, 12). The killing process is via a granule-dependent mechanism involving perforin, which is produced in activated T cells (13, 14). Therefore, both $CD4^+$ T cells and $CD8^+$ T cells, specifically of the memory phenotype capable of responding immediately to *M. tuberculosis*-infected cells, are key elements in host defenses against *M. tuberculosis*, and vaccinating agents are required to have the ability to activate T cells to produce memory subpopulations. BCG activates naive $CD4^+$ T cells substantially but not convincingly and activates naive $CD8^+$ T cells poorly (15, 16). The reasons why BCG cannot prevent the development of tuberculosis have not been elucidated fully, but one of the major reasons is its poor immunostimulatory activities, based on the lack of ability to induce phagosomal maturation (17–19). Therefore, BCG-derived antigens (Ags) cannot be fully processed in the Ag-presenting cells (APCs) and cannot be efficiently presented to $CD4^+$ T cells and $CD8^+$ T cells. These observations indicate that improvement of BCG in terms of activation ability is necessary.

Various molecules, including early secretory antigenic target 6 (ESAT6), the Ag85 family proteins, and polyprotein Mtb72F, have been identified as good candidates for component vaccines against tuberculosis (9, 20–24). However, the development of a fully reliable vaccine using these component molecules has not been successful. Furthermore, the strategy that is necessary to improve BCG is still not fully determined, although some candidate recombinant BCG (rBCG) is already available (17–19). Previously, Grode et al. produced urease-deficient rBCG that produced acidic phagosomes due to lack of ammonium production and effectively translocated into lysosomes (18). However, the urease depletion alone potentiated the immunostimulatory activity of BCG but did not effectively inhibit the multiplication of *M. tuberculosis* in lung. This requires secretion of another foreign Ag, listeriolysin. We independently produced urease-deficient rBCG (BCG-ΔUT-11-3) by depleting the *ureC* gene, which encodes urease, from parent BCG (19). BCG-ΔUT-11-3 strongly activated naive human $CD4^+$ T cells to produce IFN-γ but failed to stimu-

Received 8 September 2013 Returned for modification 1 October 2013
Accepted 18 October 2013
Published ahead of print 23 October 2013
Editor: W. R. Waters
Address correspondence to Masahiko Makino, mmaki@nih.go.jp.
Copyright © 2014, American Society for Microbiology. All Rights Reserved.
doi:10.1128/CVI.00564-13

Downloaded from http://cvi.asm.org/ on January 1, 2014 by NATL INST OF INFECTIOUS DISEAS

late naive human $CD8^+$ T cells, which indicates that another modification of BCG is necessary.

Similarly, a new reliable vaccine is needed for prevention of leprosy, which is caused by infection with *Mycobacterium leprae*. We are currently developing a new rBCG capable of inhibiting the multiplication of *M. leprae in vivo*. First, we identified major membrane protein II (MMP-II) (gene name, *bfrA* or ML2038) as one of the immunodominant Ags of *M. leprae* (25). MMP-II can ligate Toll-like receptor 2 (TLR2) and consequently activates the NF-κB pathway of APCs (25), and MMP-II-pulsed DCs activate both naive $CD4^+$ T cells and naive $CD8^+$ T cells (25, 26). Second, we tried to improve BCG by overexpressing MMP-II. When we introduced the MMP-II gene into BCG extrachromosomally, the rBCG showed enhanced activity to stimulate naive T cells of both CD4 and CD8 subsets (27). The second rBCG that we produced was BCG-70M, having a BCG-derived heat shock protein 70 (HSP70)-MMP-II fusion gene, and subcutaneous single BCG-70M vaccination inhibited the multiplication of *M. leprae* in C57BL/6 mice (28). Therefore, the secretion of the HSP70-MMP-II fusion protein was useful for enhancing the T cell-stimulating activity of BCG.

Overall, these results suggest that the combination of urease depletion and intraphagosomal secretion of antigenic protein is useful for construction of a new rBCG. We found that *M. tuberculosis* has an MMP-II gene (gene name, Rv1876) that is 100% homologous to the MMP-II gene of BCG and 90% homologous to that of *M. leprae* at the amino acid level. Previously, we purified the recombinant MMP-II (rMMP-II) protein of *M. tuberculosis* using *Mycobacterium smegmatis* and evaluated its immunostimulatory activities (29). Similar to *M. leprae*-derived MMP-II, *M. tuberculosis*-derived MMP-II ligates TLR2 and activates DCs, and the MMP-II-pulsed DCs activate both subsets of naive T cells (29). Furthermore, both human DCs and macrophages infected with *M. tuberculosis* strains such as H37Rv and H37Ra expressed MMP-II derivatives on their surfaces (29). These results indicate that the MMP-II of *M. tuberculosis* is highly immunogenic and might be a good candidate for vaccine development. Therefore, in this study, we produced a new rBCG, termed BCG-DHTM, in which urease-deficient BCG-ΔUT-11-3 was introduced with a fusion gene composed of the *M. tuberculosis*-derived MMP-II gene and the HSP70 gene of *M. tuberculosis* (Rv0350), and we evaluated its immunostimulatory activities.

MATERIALS AND METHODS

Preparation of cells and Ags. Peripheral blood samples were obtained from healthy purified protein derivative (PPD)-positive individuals, with informed consent. In Japan, BCG vaccination is compulsory for children (0 to 1 year of age). Peripheral blood mononuclear cells (PBMCs) were isolated using Ficoll-Paque Plus (GE Healthcare, Uppsala, Sweden) and cryopreserved in liquid nitrogen until use, as described previously (30). For the preparation of peripheral monocytes, $CD3^+$ T cells were removed from either freshly isolated heparinized blood or cryopreserved PBMCs by using immunomagnetic beads coated with anti-CD3 monoclonal antibody (MAb) (Dynabeads 450; Dynal Biotech, Oslo, Norway). The $CD3^-$ PBMC fraction was plated on tissue culture plates, and adherent cells were used as monocytes (31). DCs were differentiated as described previously (30, 32). Briefly, monocytes were cultured in the presence of 50 ng of recombinant granulocyte-macrophage colony-stimulating factor (rGM-CSF) (Pepro Tech EC Ltd., London, England) and 10 ng of recombinant interleukin-4 (rIL-4) (Pepro Tech) per ml (32). On day 4 of culture, immature DCs were infected with rBCG at the indicated multiplicity of infection (MOI) and, on day 6 of culture, DCs were used for further analyses of surface Ag and for mixed lymphocyte assays. Macrophages were differentiated as described previously (33, 34). In brief, monocytes were cultured in the presence of 10 ng of recombinant macrophage colony-stimulating factor (rM-CSF) (R&D Systems, Inc., Minneapolis, MN) per ml. On day 5 of culture, macrophages were infected with rBCG at the indicated MOIs and, on day 7 of culture, they were used for further analyses of surface Ag and for mixed lymphocyte assays. The rMMP-II protein was produced as described previously (25, 35). The rHSP70 protein was purchased (Hy Test Ltd., Turku, Finland), and H37Rv-derived cytosolic protein was produced as described previously (35).

Vector construction and preparation of rBCG. The genomic DNAs were obtained from BCG substrain Tokyo and from *M. tuberculosis* strain H37Rv. The oligonucleotide primers used for amplification of the *hsp70* gene were F-Mb70Bal (5′-aaaTGGCCAtggctcgtgcggtcggg-3′) and R-Mb70Eco (5′-aaaGAATTCcttggcctcccggccg-3′). The MMP-II sequence from *M. tuberculosis* genomic DNA was amplified with primers F-MMPTBEco (5′-aattGAATTCatgcaaggtgatcccgatgt-3′) and R-MMPT-BSal (5′-aattGTCGACtcaggtcggtgggcgaga-3′). In all primer sequences, capital letters indicate restriction sites. The amplified products were digested with appropriate restriction enzymes and cloned into the parental pMV261 plasmid. For replacement of the kanamycin resistance gene with the hygromycin resistance cassette, the XbaI-NheI fragment from pYUB854 (36) was cloned into the SpeI-NheI fragment of the plasmid (36). The rBCG in which the *ureC* gene was disrupted (BCG-ΔUT-11) was produced as described previously (19). The hygromycin cassette in BCG-ΔUT-11 was removed by using pYUB870 encoding γδ-resolvase (γδ-*tnp*R) (36). The unmarked BCG was named BCG-ΔUT-11-3. The HSP70-MMP II fusion protein-expressing vector was introduced into BCG-ΔUT-11-3 by electroporation. BCG-ΔUT-11-3 containing pMV-HSP70-MMP-II as an extrachromosomal plasmid is referred to as BCG-DHTM, and BCG-Tokyo containing pMV-261-hygromycin is referred to as BCG-261H (BCG vector control). Recombinant BCGs and *M. tuberculosis* strain H37Rv were grown to log phase and stored at −80°C, at 10^8 CFU/ml. Before infection of DCs and macrophages, BCG levels were counted by the colony assay method. There was no significant difference in *in vitro* culture growth between BCG-261H and BCG-DHTM.

Analysis of cell surface Ags. The expression of cell surface Ags on DCs and lymphocytes was analyzed using a FACSCalibur system (BD Biosciences, San Jose, CA). Dead cells were eliminated from the analysis by staining with propidium iodide (Sigma-Aldrich, St. Louis, MO), and 1×10^4 live cells were analyzed. For the analysis of cell surface Ags, the following MAbs were used: fluorescein isothiocyanate (FITC)-conjugated MAbs against HLA-ABC (G46-2.6; BD Biosciences), HLA-DR (L243; BD Biosciences), CD86 (FUN-1; BD Biosciences), CD83 (HB15a; Immunotech, Marseille, France), CD62L (Dreg 56; BD Biosciences), CCR7 (clone 150503; R&D Systems), and CD27 (M-T271; BD Biosciences) and phycoerythrin-conjugated MAbs to CD162 (TB5; Exbio, Prague, Czech Republic), CD8 (RPA-T8; BD Biosciences), and CD4 (RPA-T4; BD Biosciences).

The expression of MMP-II on rBCG-infected DCs was determined using the MAb against MMP-II of *M. leprae* (M270-13, IgM, kappa), which may detect MMP-II associated with major histocompatibility complex (MHC) molecules (26), followed by FITC-conjugated anti-mouse immunoglobulin (Ig) MAb (Tago Immunologicals, Camarillo, CA). For inhibition of the intracellular processing of phagocytosed bacteria, DCs were treated with 50 μM chloroquine (Sigma-Aldrich) for 2 h, washed, infected with rBCG, and subjected to analyses of MMP-II surface expression. The intracellular production of perforin was assessed as follows: naive $CD8^+$ T cells were stimulated with rBCG-infected DCs for 5 days in the presence of naive $CD4^+$ T cells, and $CD8^+$ T cells were surface stained with phycoerythrin-labeled MAb to CD8 and fixed in 2% formaldehyde. Subsequently, the cells were permeabilized using permeabilizing solution (BD Biosciences) and were stained with FITC-conjugated MAb to perforin (δG9; BD Biosciences) or FITC-labeled isotype control.

Downloaded from http://cvi.asm.org/ on January 1, 2014 by NATL INST OF INFECTIOUS DISEAS

APC functions of DCs. The ability of BCG-infected DCs and macrophages to stimulate T cells was assessed using an autologous APC-T cell coculture, as previously described (32, 37). Purification of $CD4^+$ and $CD8^+$ T cells was conducted by using negative-isolation kits (Dynabeads 450; Dynal Biotech) (32). Naive $CD4^+$ and $CD8^+$ T cells were produced by further treatment of these T cells with MAb to CD45RO, followed by beads coated with goat anti-mouse IgG MAb (Dynal Biotech). More than 98% of $CD45RA^+$ T cells were positive for the expression of CCR7 molecules. Memory-type T cells were similarly produced by the treatment of cells with MAb to CD45RA Ag. The purified responder cells (1×10^5 cells per well) were plated in 96-well round-bottom tissue culture plates, and DCs or macrophages infected with rBCG were added to give the indicated APC/T cell ratio. Supernatants of APC-T cell cocultures were collected on day 4, and cytokine levels were determined. In some cases, rBCG-infected DCs and macrophages were treated with MAb to HLA-ABC (W6/32, mouse IgG2a, kappa), HLA-DR (L243, mouse IgG2a, kappa), or CD86 (IT2.2, mouse IgG2b, kappa; BD Biosciences) or normal mouse IgG. The optimal concentrations of the MAbs were determined in advance. Also, in some cases, immature DCs and macrophages were treated with the indicated doses of chloroquine, brefeldin A (Sigma-Aldrich), or lactacystin (Sigma-Aldrich) and subsequently infected with BCG-DHTM. The optimal doses of these reagents were determined in advance.

Measurement of cytokine production. Levels of the following cytokines were measured: IFN-γ produced by $CD4^+$ and $CD8^+$ T cells and interleukin 12p70 (IL-12p70), tumor necrosis factor alpha (TNF-α), IL-1β, and GM-CSF produced by DCs or macrophages stimulated for 24 or 48 h with rBCGs. The concentrations of these cytokines were quantified using enzyme assay kits (Opt EIA human enzyme-linked immunosorbent assay [ELISA] set; BD Biosciences).

Animal studies. For inoculation into mice, rBCG and *M. tuberculosis* strain H37Rv were cultured in Middlebrook 7H9 medium to log phase and stored at −80°C, at 10^8 CFU/ml. Before the aliquots were used for inoculation, the concentrations of viable bacilli were determined by plating on Middlebrook 7H10 agar plates. Three 5-week-old C57BL/6J mice (Clea Japan Inc., Tokyo, Japan) per group were inoculated subcutaneously with 0.1 ml of phosphate-buffered saline (PBS) or PBS containing 1×10^3 or 1×10^4 rBCG. The animals were kept under specific pathogen-free conditions and were supplied with sterilized food and water. Four or 12 weeks after inoculation, the spleens were removed and splenocytes were suspended in culture medium at a concentration of 2×10^6 cells per ml. The splenocytes were stimulated with the indicated concentrations of rMMP-II, rHSP70 (HyTest), or H37Rv-derived cytosolic protein, in triplicate, in 96-well round-bottom microplates (19, 27). The individual culture supernatants were collected 3 to 4 days after stimulation. For observation of the effect of BCG vaccination on *M. tuberculosis* infection, five C57BL/6 mice per group were vaccinated with either BCG-261H or BCG-DHTM, at 1×10^4 CFU/mouse, for 6 weeks and were challenged with H37Rv at 100 CFU/lung by aerosol infection using an automated inhalation exposure apparatus (model 099C A4212; Glas-Col Corp.). Six weeks later, bacterial burdens in the lung and spleen were assessed by mechanical disruption in PBS with 0.5% (vol/vol) Tween 80 and enumerated by colony assay. Animal studies were reviewed and approved by the Animal Research Committee of Experimental Animals of the National Institute of Infectious Diseases and were conducted according to their guidelines.

Statistical analysis. Student's *t* test was applied to determine statistical differences. Throughout the *in vitro* experiments, we included 1 or 2 technical replicates in each individual experiment and used at least 3 separate PBMC donors.

RESULTS

Activation of Ag-presenting cells by BCG-DHTM. The purpose of rBCG production is to activate naive T cells effectively and, consequently, to produce memory-type T cells efficiently. In order to stimulate responder T cells, APCs susceptible to BCG infection should be adequately activated by infection with rBCG. We assessed the ability of newly produced rBCG (BCG-DHTM) to activate APCs with respect to phenotypic changes and cytokine production (Fig. 1). To assess phenotypic changes, we examined the expression of MHC, CD86, and CD83 molecules on DCs (Fig. 1a). Both vector control BCG (BCG-261H) and BCG-DHTM upregulated the expression of these molecules, but BCG-DHTM infection induced upregulation more efficiently than did infection with BCG-261H. We measured the production of cytokines, including IL-12p70, TNF-α, and IL-1β, from DCs with stimulation with rBCGs (Fig. 1b). Significantly higher levels of all of these cytokines were produced by BCG-DHTM stimulation. Further, when M-CSF-dependent macrophages were stimulated with either BCG-261H or BCG-DHTM, BCG-DHTM stimulation induced production of significantly higher levels of TNF-α and GM-CSF (Fig. 1c). In all of these experiments, we used various doses of rBCGs for the assessments, and similar changes were observed (data not shown). These results indicated that BCG-DHTM activated DCs and macrophages more efficiently than did BCG-261H.

Activation of memory-type and naive $CD4^+$ T cells by BCG-DHTM. Previously, we reported that the enhanced activation of both $CD4^+$ T cells and $CD8^+$ T cells induced by rBCG that was introduced with the *M. leprae*-derived MMP-II-HSP70 fusion gene was dependent on secretion of the HSP70-MMP-II fusion protein. Since we also confirmed that newly produced BCG-DHTM secreted the fusion protein composed of *M. tuberculosis*-derived MMP-II and HSP70 (data not shown), we assessed the $CD4^+$ T cell-stimulating ability of BCG-DHTM (Fig. 2). When either BCG-261H or BCG-DHTM was used to infect DCs and was used as a stimulator, autologous memory-type $CD4^+$ T cells produced significantly higher levels of IFN-γ by stimulation of BCG-DHTM-infected DCs than BCG-261H-infected DCs (Fig. 2a); around 300 pg/ml of IFN-γ was secreted by stimulation with very small numbers of rBCG-infected DCs (MOI, 0.063) and with very small numbers of DCs (T cell/DC ratio, 80:1). At different T cell/DC ratios, BCG-DHTM exhibited higher activity (data not shown). In addition to IFN-γ, TNF-α and IL-2 were efficiently produced with BCG-DHTM stimulation (data not shown). Then, we assessed rBCG-infected macrophages as stimulators. Compared to DCs, macrophages needed to be infected with higher doses of rBCGs to stimulate memory-type $CD4^+$ T cells; however, more than 100 pg/ml of IFN-γ could be produced by responder $CD4^+$ T cells when BCG-DHTM was used at an MOI of 0.5 to infect macrophages. Further, a larger quantity of macrophages (T cell/macrophage ratio, 10:1) was needed to activate $CD4^+$ T cells convincingly (Fig. 2b). It should be noted that the BCG vector control could not induce the apparent activation of $CD4^+$ T cells. BCG-DHTM did not induce IFN-γ production from either DCs or macrophages (data not shown). Then, we assessed the activity of BCG-DHTM to stimulate naive $CD4^+$ T cells (Fig. 2c). BCG-DHTM induced the production of significantly higher levels of IFN-γ than did BCG-261H at MOIs of 0.063 to 0.25 (T cell/DC ratio, 20:1). Increasing IFN-γ levels could be produced, depending on the dose of BCG-DHTM used to infect DCs. Also, at different T cell/DC ratios, BCG-DHTM showed greater activity (data not shown). However, BCG-DHTM-infected macrophages failed to induce the production of significant levels of IFN-γ from naive $CD4^+$ T cells or $CD8^+$ T cells (data not shown).

Activation of memory-type and naive $CD8^+$ T cells by BCG-DHTM. The effects of BCG-DHTM-infected DCs on $CD8^+$ T cell activation were examined (Fig. 3). While BCG-261H did not ac-

Downloaded from http://cvi.asm.org/ on January 1, 2014 by NATL INST OF INFECTIOUS DISEAS

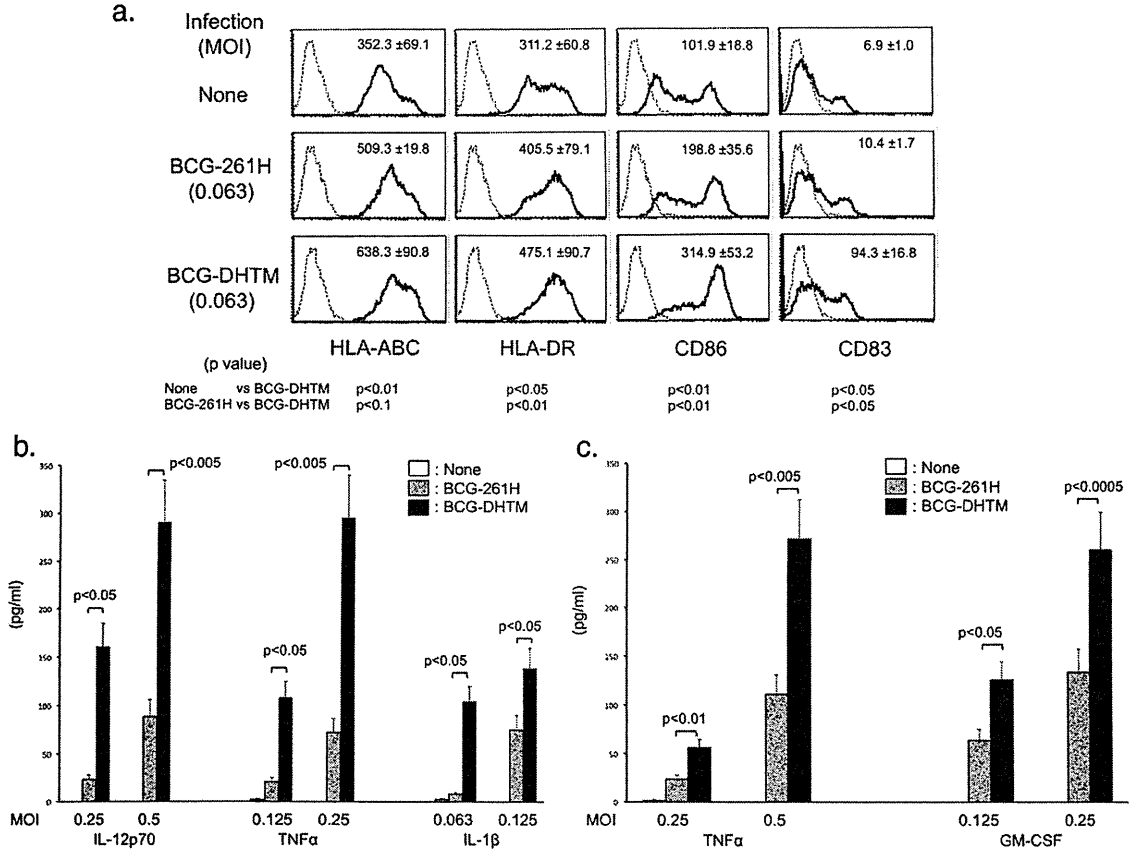

FIG 1 (a) Upregulation of APC-associated molecules and activation markers on DCs by infection with BCG-DHTM. Monocyte-derived immature DCs were infected with either BCG-261H or BCG-DHTM at an MOI of 0.063 and were cultured for another 2 days in the presence of rGM-CSF and rIL-4. The DCs from day 6 of culture were gated and analyzed. Dashed lines, isotype-matched control IgG; solid lines, indicated test MAbs. Representative results of three separate experiments are shown. The numbers in the top right corners of the panels represent the differences in fluorescence intensity (mean ± standard deviation [SD]) between the control IgG and the test MAb in three independent experiments. (b) Cytokine production from DCs by stimulation with BCG-DHTM. DCs produced using rGM-CSF and rIL-4 were stimulated with either BCG-261H or BCG-DHTM for 24 h. (c) Cytokine production from macrophages by stimulation with BCG-DHTM. Macrophages differentiated from monocytes by using M-CSF were stimulated with either BCG-261H or BCG-DHTM for 24 h. The concentrations of the indicated cytokines were determined by the ELISA method. A representative of three separate experiments is shown. Assays were performed in triplicate, and the results are expressed as mean ± SD. Titers were statistically compared using Student's *t* test.

tivate memory $CD8^+$ T cells efficiently, BCG-DHTM activated the T cells and induced the production of more than 100 pg/ml of IFN-γ (Fig. 3a). Compared to the dose of rBCG required for activation of memory-type $CD4^+$ T cells, a higher dose of rBCG was needed, which may be based on the fact that parent BCG did not activate naive $CD8^+$ T cells and did not produce BCG-specific memory-type $CD8^+$ T cells efficiently. When autologous naive $CD8^+$ T cells were stimulated by rBCG as a responder population, only BCG-DHTM efficiently activated naive $CD8^+$ cells to produce IFN-γ (Fig. 3b). Efficient concentrations of IFN-γ could be produced from naive $CD8^+$ T cells by stimulation with DCs infected with BCG-DHTM. As observed previously (18, 32), BCG-261H did not activate naive $CD8^+$ T cells. These phenomena were observed consistently under various conditions, including different MOIs and T cell/DC ratios. In order to confirm the activation of naive $CD8^+$ T cells by BCG-DHTM, the expression of activation markers on naive $CD8^+$ T cells was examined (Fig. 3c). When autologous naive $CD8^+$ T cells were stimulated with DCs infected with either BCG-261H or BCG-DHTM in the presence of naive $CD4^+$ T cells, more-efficient downregulation of CD62L expression on $CD8^+$ T cells was induced by BCG-DHTM stimulation. These phenomena were observed at different MOIs and, even at lower MOIs such as 0.031, efficient downregulation was observed in BCG-DHTM-stimulated $CD8^+$ T cells.

Characteristics of BCG-DHTM. Previously, we reported that BCG-70M induced expression of MMP-II on the surface of DCs infected with BCG-70 M (28). Thus, we analyzed the DCs infected with BCG-DHTM in terms of MMP-II expression (Fig. 4a). Whereas both uninfected DCs and DCs infected with BCG-261H did not express MMP-II derivatives on the surface, BCG-DHTM induced expression of MMP-II derivatives (6.8-fold increase in MMP-II expression in BCG-261H-infected DCs). Higher levels of expression were observed when higher MOIs of rBCG were used (data not shown). Further, MMP-II expression was inhibited by the treatment of immature DCs with chloroquine, an inhibitor of phagosomal acidification, prior to infection with BCG-DHTM.

Downloaded from http://cvi.asm.org/ on January 1, 2014 by NATL INST OF INFECTIOUS DISEAS

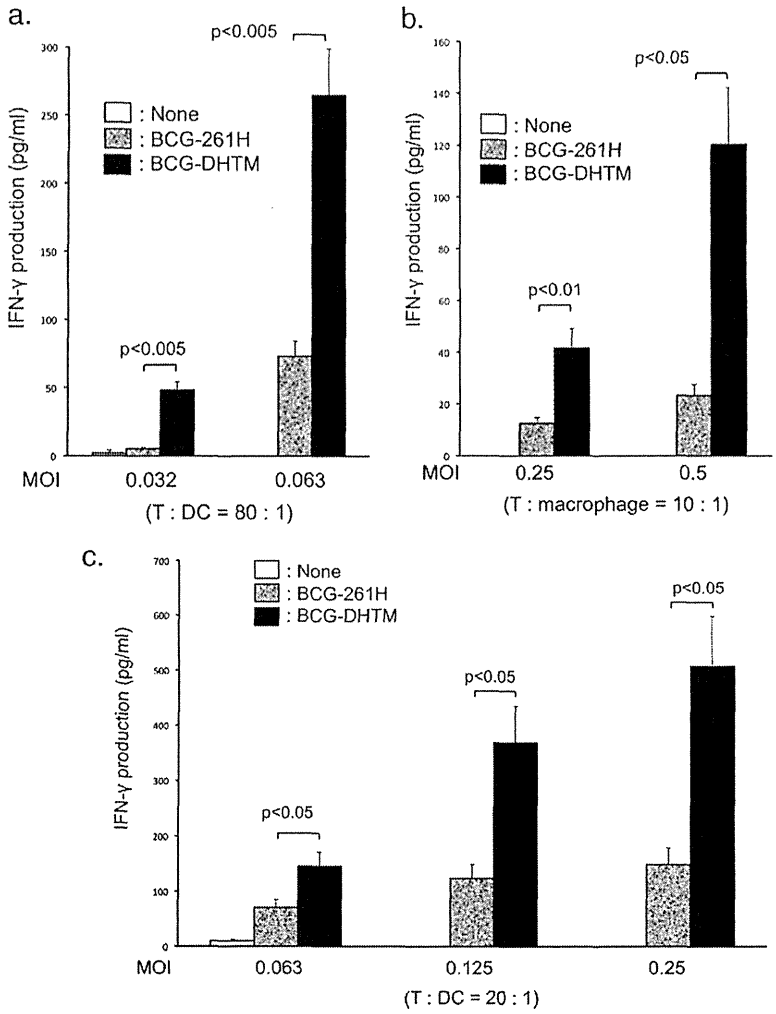

FIG 2 (a) IFN-γ production from memory-type $CD4^+$ T cells by stimulation with BCG-DHTM-infected DCs. Monocyte-derived DCs were infected with either BCG-261H or BCG-DHTM at the indicated MOIs and were used as stimulators of memory-type $CD4^+$ T cells in a 4-day culture; 10^5 responder T cells were stimulated with the rBCG-infected DCs at a T cell/DC ratio of 80:1. (b) IFN-γ production from memory-type $CD4^+$ T cells by stimulation with BCG-DHTM-infected macrophages. Macrophages produced by using M-CSF were infected with either BCG-261H or BCG-DHTM at the indicated MOIs and were used as stimulators of responder $CD4^+$ T cells in a 4-day culture; 10^5 responder T cells were stimulated with the rBCG-infected macrophages at a T cell/macrophage ratio of 10:1. (c) IFN-γ production from naive $CD4^+$ T cells by stimulation with BCG-DHTM-infected DCs. Monocyte-derived DCs were infected with either BCG-261H or BCG-DHTM at the indicated MOIs and were used as stimulators; 10^5 responder naive $CD4^+$ T cells were stimulated with the rBCG-infected DCs at a T cell/DC ratio of 20:1. A representative of three separate experiments is shown. Assays were performed in triplicate, and the results are expressed as mean ± SD. Titers were statistically compared using Student's *t* test.

According to these results, we analyzed the effect of chloroquine treatment of immature DCs on the activation of T cells by BCG-DHTM (Fig. 4b). IFN-γ production from naive $CD4^+$ T cells and naive $CD8^+$ T cells by stimulation with BCG-DHTM-infected DCs and that from memory-type $CD4^+$ T cells by stimulation with BCG-DHTM-infected macrophages were significantly inhibited by chloroquine treatment of these APCs. These results suggest the possibility that the secreted fusion protein is one of the elements responsible for the activation of both $CD4^+$ T cells and $CD8^+$ T cells. BCG-DHTM-infected DCs or macrophages were treated with MAbs to HLA and CD86 molecules prior to being used as stimulators of responder T cells (Fig. 4c). Treatment of BCG-DHTM-infected APCs with MAbs to HLA-DR, CD86, and MMP-II (data not shown) significantly inhibited IFN-γ production from naive $CD4^+$ T cells and memory-type $CD4^+$ T cells. Also, the treatment of BCG-DHTM-infected DCs with MAbs to HLA-ABC and CD86 molecules significantly inhibited the production of IFN-γ from naive $CD8^+$ T cells. These results suggested that BCG-DHTM activated T cells in an Ag-specific manner, at least partially. In general, for activation of naive $CD8^+$ T cells by bacteria, the activation of cross-presenting pathways in APCs is required. We examined whether BCG-DHTM utilized the cytosolic cross-presentation pathway for the activation of naive $CD8^+$ T cells (Fig. 4d). To this end, we treated immature DCs with either

Downloaded from http://cvi.asm.org/ on January 1, 2014 by NATL INST OF INFECTIOUS DISEAS

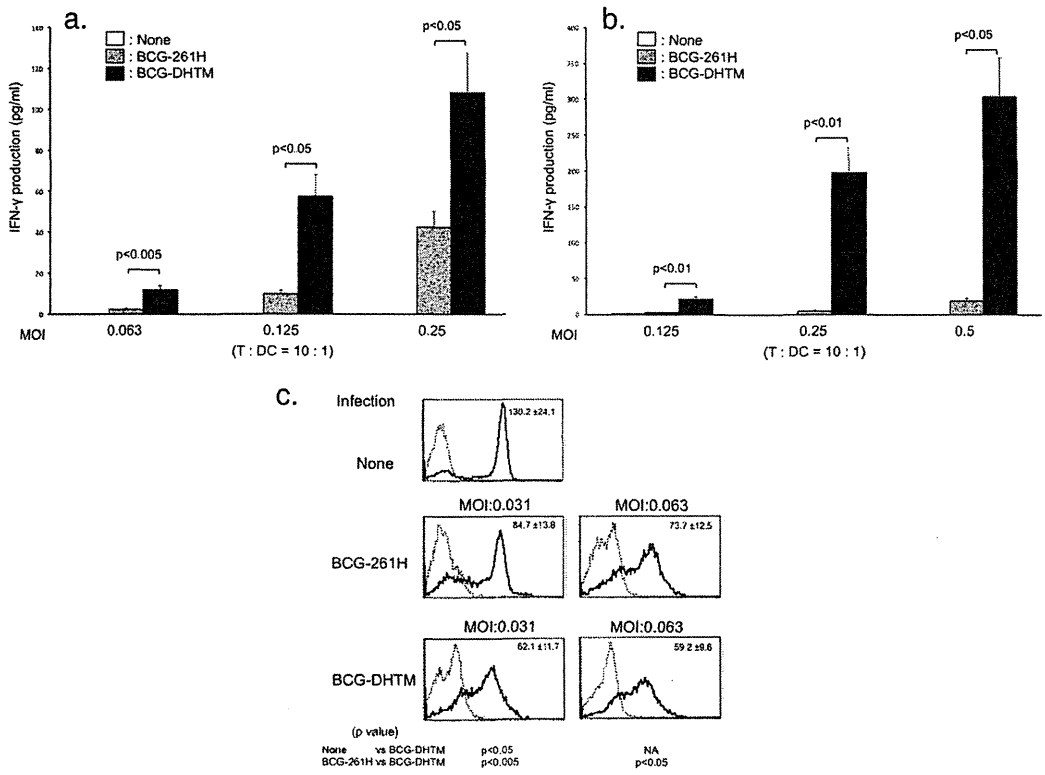

FIG 3 (a) IFN-γ production from memory-type $CD8^+$ T cells by stimulation with BCG-DHTM. Monocyte-derived DCs were infected with either BCG-261H or BCG-DHTM at the indicated MOIs and were used as stimulators; 10^5 responder memory-type $CD8^+$ T cells were stimulated for 4 days with rBCG-infected DCs at a T cell/DC ratio of 10:1. (b) IFN-γ production from naive $CD8^+$ T cells by stimulation with BCG-DHTM. DCs were infected with either BCG-261H or BCG-DHTM at the indicated MOIs and were used as stimulators; 10^5 responder T cells were stimulated for 4 days with rBCG-infected DCs at a T cell/DC ratio of 10:1. A representative of three separate experiments is shown. Assays were performed in triplicate, and the results are expressed as mean ± SD. Titers were statistically compared using Student's *t* test. (c) Downregulation of CD62L expression on naive $CD8^+$ T cells by BCG-DHTM stimulation. DCs were infected with either BCG-261H or BCG-DHTM at the indicated MOIs and were cocultured with unseparated naive T cells for 5 days at a T cell/DC ratio of 20:1. The stimulated $CD8^+$ T cells were gated and analyzed for expression of CD62L molecules. Dashed lines, isotype-matched control IgG; solid lines, anti-CD62L MAb. The numbers in the top right corners of the panels represent the differences in fluorescence intensity (mean ± standard deviation) between the control IgG and anti-CD62L MAb in three independent experiments. A representative of three separate experiments is shown.

brefeldin A or lactacystin and subsequently infected them with BCG-DHTM at an MOI of 0.25. These pretreatments of DCs significantly inhibited IFN-γ production from naive $CD8^+$ T cells.

Production of memory and effector T cells from naive $CD8^+$ T cells by BCG-DHTM. Since it is well documented that the production of long-lasting memory $CD8^+$ T cells from naive $CD8^+$ T cells requires help from $CD4^+$ T cells and since BCG-DHTM activated both naive $CD4^+$ T cells and naive $CD8^+$ T cells, naive unseparated T cells were stimulated with DCs infected with either BCG-261H or BCG-DHTM and the stimulated $CD8^+$ T cells were gated and analyzed (Fig. 5a). Stimulation with BCG-DHTM more efficiently produced $CD27^{low}$ or $CCR7^{low}$ memory-type T cells from naive T cells. Further, BCG-DHTM produced perforin-producing $CD8^+$ T cells more efficiently than did BCG-261H. Efficient production of these $CD8^+$ T cells was observed with different doses of BCG; however, in the absence of $CD4^+$ T cells, production of memory and effector T cells was not observed (data not shown). Furthermore, it is necessary to produce T cells with high migratory function. Thus, we assessed the expression of CD162 on both $CD4^+$ T cells and $CD8^+$ T cells stimulated with DCs infected with BCG-DHTM (Fig. 5b). BCG-DHTM produced $CD162^{high}$ $CD4^+$ T cells and $CD162^{high}$ $CD8^+$ T cells more efficiently than did BCG-261H. Similar differences between BCG-261H and BCG-DHTM were observed at different MOIs (data not shown).

Production of T cells responsive to secondary stimulation by BCG-DHTM infection *in vivo*. Functional studies using C57BL/6 mice were conducted to examine the ability of BCG-DHTM to produce T cells that were highly responsive to secondary *in vitro* stimulation (Fig. 6). The mice were subcutaneously inoculated with 1×10^3 CFU/mouse of rBCGs 4 weeks (Fig. 6a) or 12 weeks (Fig. 6b) before *in vitro* stimulation. As secondary stimulators, recombinant MMP-II, recombinant HSP70 protein, and H37Rv-derived cytosolic protein were used. Some of these proteins are highly immunogenic and thus they induced substantial IFN-γ production from T cells of uninfected mice; however, splenic T cells from mice inoculated with BCG-DHTM 4 weeks previously produced significantly higher levels of IFN-γ and IL-2 (data not shown) than did T cells from uninoculated mice and those from BCG-261H-infected mice, by responding to all of the secondary stimulators (Fig. 6a). To examine the long-term effects of single inoculations of BCG-DHTM, T cells from C57BL/6 mice similarly

Downloaded from http://cvi.asm.org/ on January 1, 2014 by NATL INST OF INFECTIOUS DISEAS

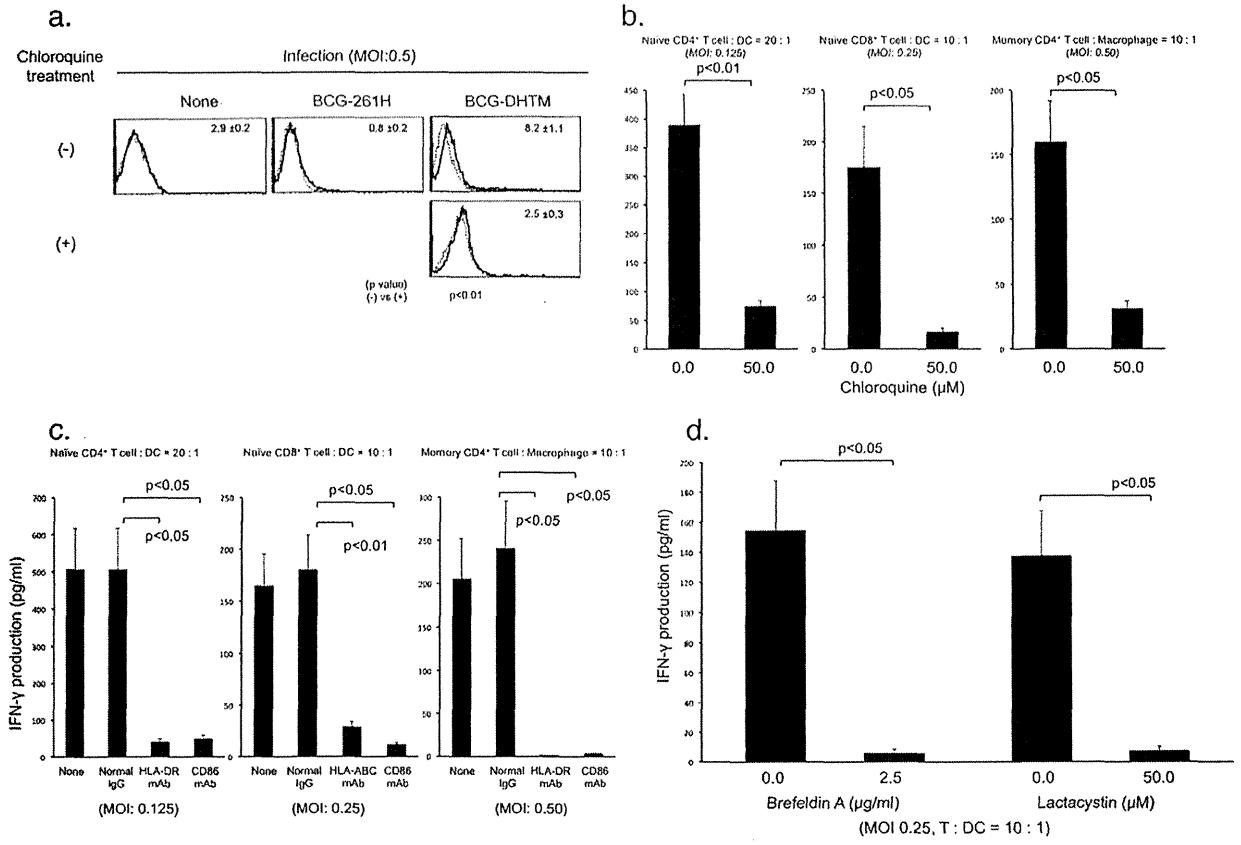

FIG 4 (a) Expression of MMP-II on DCs. Immature DCs were either treated with 50 μM chloroquine for 2 h or not treated and subsequently were infected with either BCG-261H or BCG-DHTM at an MOI of 0.5. After 2 days of culture in the presence of rGM-CSF and rIL-4, DCs were gated and analyzed. Dashed lines, control normal IgM; solid lines, anti-MMP-II MAb (IgM). The numbers in the top right corners of the panels represent the differences in fluorescence intensity (mean ± standard deviation) between the control IgM and MMP-II MAb in three independent experiments. Representative results of three separate experiments are shown. (b) Effects of chloroquine treatment of DCs and macrophages on the activation of T cells. Immature DCs and macrophages were treated with chloroquine (50 μM for 2 h) or not treated and subsequently were infected with BCG-DHTM at the indicated MOIs. These DCs and macrophages were used as stimulators of the indicated responder T cells at the indicated responder/stimulator ratios. IFN-γ produced by T cells was measured. (c) Inhibition of T cell activation by treatment of BCG-DHTM-infected DCs and macrophages with MAbs. DCs and macrophages were infected with BCG-DHTM at the indicated MOIs and subsequently were treated with 10 μg/ml of the MAb or normal murine IgG. These APCs were used as the stimulators of the indicated responder T cells (1×10^5 cells/well), at the indicated T cell/APC ratios, for 4 days. IFN-γ produced by T cells was measured. (d) Effects of treatment of immature DCs with brefeldin A or lactacystin on the activation of naive $CD8^+$ T cells. Immature DCs from 4 days of culture were treated with either brefeldin A (2.5 μg/ml) or lactacystin (50 μM) or not treated and subsequently were infected with BCG-DHTM at an MOI of 0.25. These DCs were used as stimulators of responder autologous naive $CD8^+$ T cells (1×10^5/well) at a T cell/DC ratio of 10:1. IFN-γ produced by T cells was measured. A representative of three separate experiments is shown. Assays were performed in triplicate, and the results are expressed as mean ± SD. Titers were statistically compared using Student's *t* test.

inoculated with rBCGs 12 weeks previously were examined (Fig. 6b). Again, significantly higher levels of IFN-γ were produced from T cells obtained from mice inoculated with BCG-DHTM with secondary stimulation, although we could not recover BCG from spleen. In a separate experiment, a different dose (1×10^2 CFU/mouse) of BCG was examined, and similar results were obtained (data not shown).

Effect of BCG-DHTM vaccination on the multiplication of H37Rv *in vivo*. C57BL/6 mice vaccinated with either BCG-261H or BCG-DHTM (1×10^4 CFU/mouse) for 6 weeks were challenged with 100 CFU per lung of H37Rv by aerosol infection. Six weeks later, the *M. tuberculosis* recovered from both lungs and spleen was enumerated (Fig. 7). Mice vaccinated with either BCG-261H or BCG-DHTM demonstrated inhibited multiplication of *M. tuberculosis* in the lung, and BCG-DHTM vaccination inhibited *M. tuberculosis* multiplication more strongly than did BCG-261H vaccination (Fig. 7a). Similar results were observed in the spleen (Fig. 7b). Similar protective effects of BCG-DHTM on *M. tuberculosis* recovery were observed in mice 12 weeks after vaccination (data not shown).

DISCUSSION

Studies using the T cell receptor-transgenic *M. tuberculosis* mouse model clearly demonstrated that the most susceptible APCs, including DCs and macrophages, need at least 7 to 10 days to initiate stimulation of $CD4^+$ T cells and $CD8^+$ T cells in regional lymph nodes on aerosol infection with *M. tuberculosis* and the stimulated T cells need 4 to 5 weeks to initiate inhibition of the multiplication of *M. tuberculosis* in lungs (38). The activation of both $CD4^+$ T cells and $CD8^+$ T cells is required for inhibition of the replication

Downloaded from http://cvi.asm.org/ on January 1, 2014 by NATL INST OF INFECTIOUS DISEAS

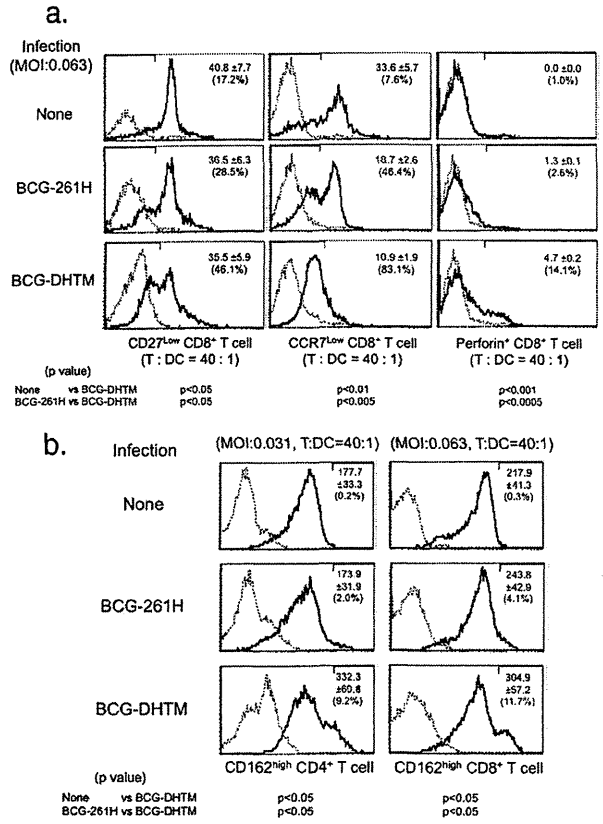

FIG 5 (a) Expression of memory markers and perforin production on naive $CD8^+$ T cells stimulated with DCs infected with BCG-DHTM. DCs were infected with either BCG-261H or BCG-DHTM at an MOI of 0.063 and were cocultured with unseparated naive T cells (T cell/DC ratio of 40:1) for 5 days. The stimulated $CD8^+$ T cells were gated and analyzed for expression of the indicated molecules and for perforin production. (b) Expression of migration markers on naive T cells. DCs were infected with either BCG-261H or BCG-DHTM at the indicated MOIs and were cocultured with naive T cells (T cell/DC ratio of 40:1) for 5 days. Stimulated T cells of the CD4 or CD8 subset were gated and analyzed for expression of CD162 molecules. Dashed lines, isotype-matched control IgG; solid lines, anti-CD162 MAb. The numbers in the top right corners of the panels represent the differences in fluorescence intensity (mean ± standard deviation) between the control IgG and the test MAb in three independent experiments. The numbers in parentheses indicate the percentages of the $CD162^{high}$ T cell population among the indicated T cells. A representative of three separate experiments is shown.

of *M. tuberculosis* or killing of *M. tuberculosis* (7–9), and DCs play a central role in activating T cells (39). It has been reported that $CD4^+$ T cells act at the initial stage of *M. tuberculosis* infection and $CD8^+$ T cells work chiefly at the chronic stage (4). The purpose of vaccination aimed at controlling tuberculosis manifestation is to produce T cells that can immediately respond to antigenic molecules expressed on the surface of *M. tuberculosis*-infected APCs in the regional lymph nodes. BCG is essentially capable of activating naive $CD4^+$ T cells, but its potency is not convincing and is not suitable for stimulation of naive $CD8^+$ T cells (15, 16). Further, macrophages infected with BCG inefficiently activate $CD4^+$ T cells (15). Therefore, BCG is not an excellent vaccine in terms of producing abundant T cells capable of responding to secondary stimulation, and improvement of BCG is necessary.

We have previously made efforts to improve the ability of BCG to stimulate T cells, chiefly aiming to produce better vaccines against leprosy. We used MMP-II protein to improve the function of BCG, as the most important element of vaccines (25), and we found that intraphagosomal secretion of HSP70-MMP-II fusion protein is quite useful to stimulate naive T cells of both CD4 and CD8 subsets. Further, we and others showed that urease-deficient rBCG feasibly translocated into lysosomes, where abundant enzymes are available (18). Although urease-deficient BCG-ΔUT-11-3 activated naive $CD4^+$ T cells, it failed to activate naive $CD8^+$ T cells to produce IFN-γ (19). Furthermore, Grode et al. showed that depletion of urease activity in BCG is not sufficient to inhibit the multiplication of *M. tuberculosis* in lung (18). Therefore, it could be speculated that, in order to overcome fully the intrinsic defect of BCG, that is, a lack of phagosome and lysosome fusion, the combination of urease depletion and intraphagosomal secretion of antigenic molecules would be useful.

Our previous study indicated that the rMMP-II protein of *M. tuberculosis* is highly immunogenic and DCs pulsed with MMP-II proteins activated both naive $CD4^+$ T cells and naive $CD8^+$ T cells, but *M. tuberculosis*-derived MMP-II was superior to *M. leprae*-derived MMP-II in all of these functions (29). Furthermore, individuals who were vaccinated with BCG possessing MMP-II 100% homologous to that of *M. tuberculosis* were assumed to be primed with MMP-II *in vivo* (29). Thus, MMP-II of *M. tuberculosis* was considered to have T cell-stimulating activity, and these activated T cells, which subsequently differentiated into the memory state, may be able to respond to *M. tuberculosis*-infected APCs immediately. Therefore, MMP-II could be a useful candidate as a component of vaccines against tuberculosis.

Based on these previous findings and speculation, we produced a new rBCG termed BCG-DHTM, using the MMP-II of *M. tuberculosis*. BCG-DHTM was produced by introducing the HSP70-MMP-II fusion gene into urease-deficient BCG-ΔUT-11-3. Previously, we reported that urease-deficient rBCG that secretes a fusion protein composed of HSP70 and MMP-II from *M. leprae* was superior to urease-deficient BCG-ΔUT-11-3 and normal BCG that secretes the fusion protein in the activation of APCs and naive T cells and the production of memory-type T cells in mice (40). Therefore, we used only vector control BCG-261H as a control BCG in this study. BCG-DHTM induced enhanced activation of naive $CD4^+$ T cells and convincingly activated naive $CD8^+$ T cells to produce IFN-γ, although the availability of non-BCG-vaccinated naive PBMCs would help to confirm these observations. Naive $CD8^+$ T cell activation was confirmed by the observation of phenotypic changes such as expression of activation markers. The activation of naive $CD8^+$ T cells was induced by using the transporter associated with antigen presentation (TAP) and the proteosome-dependent cytosolic cross-presenting pathway, because IFN-γ production from naive $CD8^+$ T cells was largely inhibited by pretreatment of immature DCs with either brefeldin A, an inhibitor of TAP-dependent transportation, or lactacystin, a proteosomal protein degradation blocker. The activation of naive T cells of the CD4 and CD8 subsets by BCG-DHTM was carried out in an Ag-specific manner, since treatment of BCG-DHTM-infected DCs with MAbs to MHC or CD86 molecules significantly inhibited IFN-γ production from naive T cells. Further, BCG-DHTM could activate $CD4^+$ T cells even when macrophages were used as APCs, the function of which is important, because the parent BCG possesses the solid defect of the

Downloaded from http://cvi.asm.org/ on January 1, 2014 by NATL INST OF INFECTIOUS DISEAS

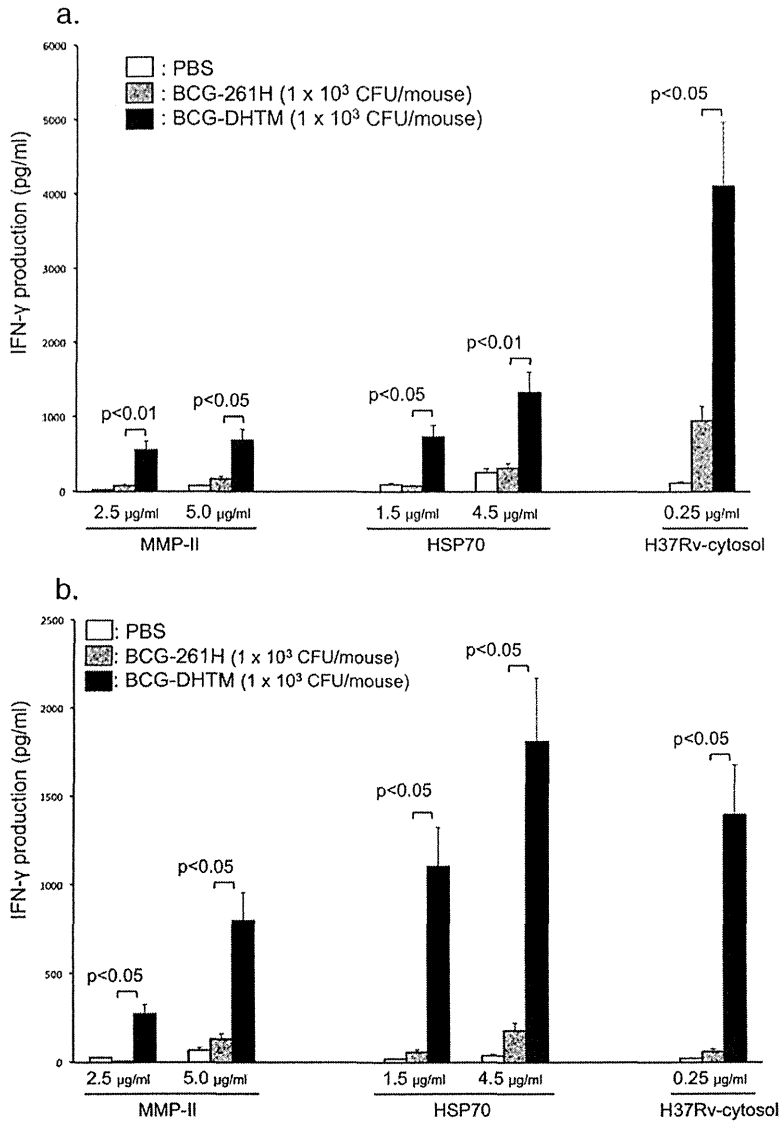

FIG 6 Production of T cells responsive to secondary *in vitro* stimulation in C57BL/6 mice by infection with BCG-DHTM. Three 5-week-old C57BL/6 mice per group were each infected subcutaneously with 1×10^3 CFU of either BCG-261H or BCG-DHTM. Four weeks (a) or 12 weeks (b) after inoculation, splenocytes (2×10^5 cells/well) were stimulated *in vitro* with the indicated stimulators for 4 days, and IFN-γ levels in the cell supernatants were measured. Assays were performed in triplicate for each mouse, and the results for three mice per group are shown as mean ± SD. Representative results of three separate experiments are shown. Concentrations of IFN-γ were statistically compared using Student's *t* test.

inability to activate $CD4^+$ T cells via macrophages. Activation of these naive T cells by DCs and activation of $CD4^+$ T cells by macrophages are closely associated with phagosomal maturation. This conclusion is supported by the observation that pretreatment of DCs and macrophages with chloroquine, an inhibitor of phagosomal acidification, blocked the activation of responder T cells. The HSP70-MMP-II fusion protein secreted in phagosomes can contribute to the activation of naive T cells but, in addition, the fusion protein can be secreted in lysosomes owing to urease deficiency. The protein secreted in lysosomes could be more efficiently degraded into antigenic determinants than that secreted in phagosomes, because lysosomes contain abundant enzymes. The frequency of T cells specific for HSP70-MMP-II fusion protein is low; thus, it seems difficult to inhibit the multiplication of *M. tuberculosis* by the actions of only the fusion protein secreted from normal rBCG. Thus, we need Ag-specific polyclonal T cells. In this respect, urease depletion seems to be useful, because rBCG itself might be processed by the enzyme present in lysosomes. Therefore, BCG-DHTM may be able to activate not only fusion protein-specific T cells but also other T cells polyclonally by using parent BCG-derived Ags. These speculations seem to be supported by animal studies, at least partially. C57BL/6 mice injected with

Downloaded from http://cvi.asm.org/ on January 1, 2014 by NATL INST OF INFECTIOUS DISEAS

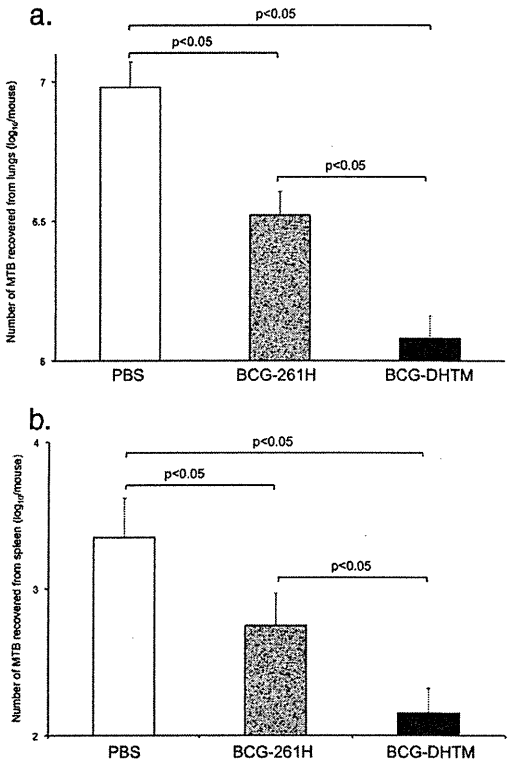

FIG 7 Inhibition of *M. tuberculosis* multiplication by subcutaneous vaccination with BCG-DHTM. Five-week-old C57BL/6 mice (5 mice/group) were subcutaneously vaccinated with either BCG-261H or BCG-DHTM at 1×10^4 CFU/mouse and were challenged with 100 CFU/lung of H37Rv by aerosol infection 6 weeks postvaccination. *M. tuberculosis* (MTB) isolates recovered from the lungs (a) and spleen (b) at 6 weeks postchallenge were enumerated by the colony assay method. Titers were statistically compared using Student's *t* test. A representative of three separate experiments is shown.

BCG-DHTM produced T cells that responded strongly to *in vitro* secondary stimulation with MMP-II and HSP70, as well as *M. tuberculosis*-derived cytosolic protein.

The BCG-DHTM stimulation of naive T cells produced $CD27^{low}$ and $CCR7^{low}$ memory-type $CD8^+$ T cells *in vitro*, and both $CD4^+$ T cells and $CD8^+$ T cells highly expressed migration markers. These observations seem to be important because both subsets of T cells have to migrate immediately and alternatively between lung and regional lymph nodes to react with *M. tuberculosis*-infected APCs efficiently. Production of these T cells may be associated with the partial inhibition of *M. tuberculosis* multiplication in lungs and spleen of mice vaccinated with BCG-DHTM. Although BCG-DHTM showed high immunostimulating activities, it only partially inhibited the growth of *M. tuberculosis* in lungs. There might be several reasons for this unconvincing inhibition. One reason might be the lack of pathogenic features of *M. tuberculosis* in BCG-DHTM, and the second is the relatively small dose of BCG used for vaccination. The third reason may be that we tested bacterial burdens in lungs and spleens at 6 weeks and not 4 weeks, a frequently used time point (41), after *M. tuberculosis* challenge, because 4 to 5 weeks are necessary to reach stable levels of pulmonary bacterial burdens even in naive mice (38). Also, due to BCG strain differences, there may be differences in protective effects in experiments with mice. Therefore, another effort is absolutely required for the production of a more potent BCG to inhibit *M. tuberculosis*. However, the present study may indicate that the HSP70-MMP-II fusion protein could be a candidate vaccine component for the control of tuberculosis.

ACKNOWLEDGMENTS

We thank M. Kujiraoka for her technical support and the Japanese Red Cross Society for kindly providing PBMCs from healthy donors.

This work was supported in part by a Grant-in-Aid for Research on Emerging and Re-emerging Infectious Diseases from the Ministry of Health, Labor, and Welfare of Japan.

REFERENCES

1. Flynn JL, Chan J. 2001. Immunology of tuberculosis. Annu. Rev. Immunol. 19:93–129. http://dx.doi.org/10.1146/annurev.immunol.19.1.93.
2. North RJ, Jung YJ. 2004. Immunity to tuberculosis. Annu. Rev. Immunol. 22:599–623. http://dx.doi.org/10.1146/annurev.immunol.22.012703.104635.
3. World Health Organization. 2012. Global tuberculosis report 2012. World Health Organization, Geneva, Switzerland.
4. Kaufmann SH, McMichael AJ. 2005. Annulling a dangerous liaison: vaccination strategies against AIDS and tuberculosis. Nat. Med. 11(Suppl):S33–S44. http://dx.doi.org/10.1038/nm1221.
5. World Health Organization. 2007. Global MDR-TB and XDR-TB response plan 2007–2008, p 1–48. *In* WHO report 2007. World Health Organization, Geneva, Switzerland.
6. Mittrücker H-W, Steinhoff U, Köhler A, Krause M, Lazar D, Mex P, Miekley D, Kaufmann SH. 2007. Poor correlation between BCG vaccination-induced T cell responses and protection against tuberculosis. Proc. Natl. Acad. Sci. U. S. A. 104:12434–12439. http://dx.doi.org/10.1073/pnas.0703510104.
7. Flynn JL, Goldstein MM, Triebold KJ, Koller B, Bloom BR. 1992. Major histocompatibility complex class I-restricted T cells are required for resistance to *Mycobacterium tuberculosis* infection. Proc. Natl. Acad. Sci. U. S. A. 89:12013–12017.
8. Hoebe K, Janssen E, Beutler B. 2004. The interface between innate and adaptive immunity. Nat. Immunol. 5:971–974. http://dx.doi.org/10.1038/ni1004-971.
9. Aagaard CS, Hoang TTKT, Vingsbo-Lundberg C, Dietrich J, Andersen P. 2009. Quality and vaccine efficacy of $CD4^+$ T cell responses directed to dominant and subdominant epitopes in ESAT-6 from *Mycobacterium tuberculosis*. J. Immunol. 183:2659–2668. http://dx.doi.org/10.4049/jimmunol.0900947.
10. Forbes EK, Sander C, Ronan EO, McShane H, Hill AVS, Beverley PCL, Tchilian EZ. 2008. Multifunctional, high-level cytokine-producing Th1 cells in the lung, but not spleen, correlate with protection against *Mycobacterium tuberculosis* aerosol challenge in mice. J. Immunol. 181:4955–4964.
11. Kaufmann SH. 1988. $CD8^+$ T lymphocytes in intracellular microbial infections. Immunol. Today 9:168–174.
12. Caccamo N, Meraviglia S, Mendola CL, Guggino G, Dieli F, Salerno A. 2006. Phenotypical and functional analysis of memory and effector human CD8 T cells specific for mycobacterial antigens. J. Immunol. 177:1780–1785.
13. Stenger S, Hanson DA, Teitelbaum R, Dewan P, Niazi KR, Froelich CJ, Ganz T, Thoma-Uszynski S, Melian A, Bogdan C, Porcelli SA, Bloom BR, Krensky AM, Modlin RL. 1998. An antimicrobial activity of cytolytic T cells mediated by granulysin. Science 282:121–125. http://dx.doi.org/10.1126/science.282.5386.121.
14. Woodworth JS, Wu Y, Behar SM. 2008. *Mycobacterium tuberculosis*-specific $CD8^+$ T cells require perforin to kill target cells and provide protection in vivo. J. Immunol. 181:8595–8603.
15. Pancholi P, Mirza A, Bhardwaj N, Steinman RM. 1993. Sequestration from immune $CD4^+$ T cells of mycobacteria growing in human macrophages. Science 260:984–986. http://dx.doi.org/10.1126/science.8098550.
16. Soualhine H, Deghmane A-E, Sun J, Mak K, Talal A, Av-Gay Y, Hmama Z. 2007. *Mycobacterium bovis* bacillus Calmette-Guérin secreting active cathepsin S stimulates expression of mature MHC class II molecules and antigen presentation in human macrophages. J. Immunol. 179:5137–5145.

Downloaded from http://cvi.asm.org/ on January 1, 2014 by NATL INST OF INFECTIOUS DISEAS